Journal of Molecular Structure 1320 (2025) 139649

Contents lists available at ScienceDirect

Journal of Molecular Structure

journal homepage: www.elsevier.com/locate/molstr

Convergent synthesis, kinetics and computational attributions of indole-*N*-phenyltriazole hybrids bearing *N*-(aryl)butanamides as alkaline phosphatase inhibitors

Shakila [a], Muhammad Athar Abbasi [a,*], Aziz-ur-Rehman [a], Sabahat Zahra Siddiqui [a], Majid Nazir [a], Hussain Raza [b], Syed Adnan Ali Shah [c,d], Daniel Moscoh Ayine-Tora [e], Muhammad Shahid [f], Song Ja Kim [b]

[a] Department of Chemistry, Government College University, Lahore 54000, Pakistan
[b] College of Natural Sciences, Department of Biological Sciences, Kongju National University, Gongju, 32588, South Korea
[c] Faculty of Pharmacy, Universiti Teknologi MARA Cawangan Selangor Kampus Puncak Alam, Bandar Puncak Alam 42300, Selangor, Malaysia
[d] Atta-ur-Rahman Institute for Natural Product Discovery (AuRIns), Universiti Teknologi MARA Cawangan Selangor Kampus Puncak Alam, Bandar Puncak Alam 42300, Selangor, Malaysia
[e] Department of Chemistry, University of Ghana, Box LG 56, Legon-Accra, Ghana
[f] Department of Biochemistry, University of Agriculture, Faisalabad 38040, Pakistan

ARTICLE INFO

Keywords:
Indole
N-Phenyltriazole
Butanamides
Alkaline phosphatase
Kinetic analysis
Hemolysis, molecular docking

ABSTRACT

In the research delineate herein, an innovative sequence of new series of multi-functional target molecules (**9a-i**) having indole-*N*-phenyltriazole bi-heterocyclic hybrids unified with *N*-arylated butanamides was synthesized as alkaline phosphatase inhibitor. The structural validation of all the formulated compounds was accomplished through IR, EI-MS, ^{1}H NMR, ^{13}C NMR and CHN analysis data. The in vitro enzyme inhibitory investigation revealed the efficacy of these bi-heterocyclic derivatives, **9a–i**, as potent inhibitors of alkaline phosphatase relative to the standard used. The compound **9h** was found to be the most active compound (IC_{50} = 0.062 ± 0.017 μM), and its inhibitory activity is about 10 times higher than potassium dihydrogen phosphate (KH_2PO_4) (IC_{50} = 5.251 ± 0.468 μM). The kinetics mechanism was attributed by evaluating the Lineweaver–Burk plots, which revealed that compound **9h** inhibited the alkaline phosphatase non-competitively to form an enzyme–inhibitor complex. The inhibition constant K_i determined from Dixon plots for this compound was 0.045 μM. The computational study was in full agreement with the experimental records and these ligands exhibited good interactions and binding energy values. These molecules also demonstrated mild cytotoxicity toward red blood cell membranes when analyzed through hemolysis. So, based on the presented results, these molecules, being the promising inhibitors of alkaline phosphatase, might be deliberated as suitable medicinal scaffolds to render normal calcification of bones and teeth.

1. Introduction

Indole, a derivative of oleum and indigo, is formed by combining the dyes oleum and indigo. It has significant biological importance and widespread occurrence in nature due to its structural versatility. It also has some interesting chemical and biological properties due to the benzo-pyrrole motif, in which the benzene and pyrrole rings are joined through the 2 and 3 positions of the pyrrole ring. Indole, being an amorphous solid by nature, has a floral aroma and is used as a base ingredient in many perfumes. Despite its dense floral aroma, the indole ring is also present as an important component in many natural products, including fungal metabolites, indole alkaloids and natural marine compounds. Due to its diverse biological activities, indole readily undergoes electrophilic aromatic substitution reactions, with the C-3 position of the pyrrole ring being the most nucleophilic, followed by the N and C-2 positions. The C-2 to C-3 double bond can often react as the alkene form. Indole can be deprotonated at the nitrogen of the pyrrole ring. The salts thus formed can be good nucleophiles. Highly ionic salts (e.g., Li^+, K^+) favor N substitution, while soft counter ions favor C-3 substitution [1].

* Corresponding author.
E-mail address: abbasi@gcu.edu.pk (M.A. Abbasi).

https://doi.org/10.1016/j.molstruc.2024.139649
Received 19 May 2024; Received in revised form 5 August 2024; Accepted 13 August 2024
Available online 14 August 2024

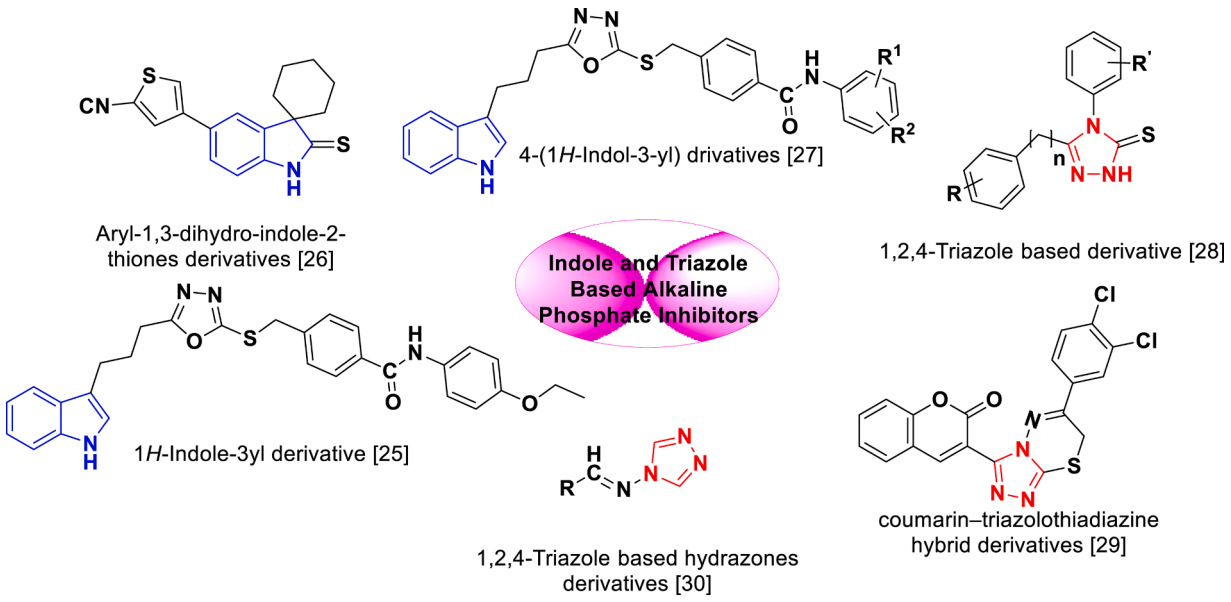

Fig. 1. Rationale of the current study.

Alkaline phosphatase is a group of isoenzymes located in the outer layer of the cell membrane. They catalyze the hydrolysis of extracellular organic phosphate esters. Zinc and magnesium are important co-factors of this enzyme. Alkaline phosphatase is present in decreasing concentrations in the placenta, ileal mucosa, kidneys, bones, and liver. Most serum alkaline phosphatase (over 80 %) is excreted by the liver and bone, and a small amount by the intestine [1,2]. Intestinal alkaline phosphatase is encoded by a separate gene, which that the gene encoding placental alkaline phosphatase and Regan isoenzyme differs [3,4]. Serum alkaline phosphatase levels increase in infancy due to bone growth and development. In the age group of 15 to 50 years, the decrease in this level is slightly higher in men than in women [5–7]. In individuals with blood groups O and B, serum alkaline phosphatase levels are increased after eating a fatty meal, due in part to the intestinal tract [8].An increase in placental alkaline phosphatase in the late third trimester leads to an increase in the number of pregnant women [9].

In recent years, compounds containing triazole rings have become potential targets for drug discovery [10–12]. The 1,2,4-triazole nucleus has emerged as one of the most influential azoles in medicinal chemistry in recent years. They have anticonvulsant, anticancer, analgesic and anti-inflammatory activities [13–16]. 1,2,4-Triazole and its derivatives are one of the most important organic compounds with industrial, agricultural, and biological activities [17]. Triazoles are known antimicrobial, antidepressant [18], anticancer [19], antimalarial [20], and anti-inflammatory [21,22] agents. Furthermore, most triazoles [23] are reported as environmentally friendly materials. Using traditional pad-dry-curing methods, the addition of triazoles to polymeric systems will improve textile materials, which is why it is also used in the development of smart and intelligent textiles [24].

From the previously reported literature, Fig. 1 [25–30], the bioactivity of triazole and indole nuclei inspired us to prepare some hybrid compounds containing indole and 1,2,4-triazole moieties embedded in a single skeleton. Thus, in continuation of our previous efforts to investigate the bioactivity of related bi-heterocyclic compounds [31], the present investigation was designed to explore some new hybrids having indole-*N*-phenyl-1,2,4-triazole core amalgamated with *N*-(aryl)butanamides as alkaline phosphate inhibitors. Additionally, the kinetic and molecular docking studies were also performed to assess their interactions with the target enzyme.

2. Experimental

The required chemicals to accomplish the targeted synthesis of hybrid molecules were purchased from Sigma Aldrich & Alfa Aesar (Germany) and solvents of Analytical grades were supplied by local suppliers. By using open capillary tube method, melting points were taken on Griffin and George apparatus and were uncorrected. By using thin layer chromatography (with ethyl acetate and *n*-hexane (30:70) as mobile phase), initial purity of compounds was detected at 254 nm. IR peaks were recorded on a Jasco-320-A spectrometer by using KBr pellet method. ^{1}H NMR signals were recorded at 600 MHz and ^{13}C NMR at 150 MHz in DMSO-d_6 using Bruker spectrometers.

2.1. Synthesis of ethyl 4-(1H-indol-3-yl)butanoate (2)

4-(1*H*-indol-3-yl)butanoic acid (0.2 mol.; **1**) dissolved in absolute ethanol (70 mL) and catalytic amount of concentrated sulfuric acid (20 mL) was taken in a 500 mL round bottom (RB) flask and refluxed for 8 h until the maximum completion of reaction, supervised through TLC. At the end, reaction mixture was neutralized with 10 % aqueous sodium carbonate (40 mL). The product was isolated by solvent extraction by chloroform (50 mL × 3). The solvent was distilled off and the required ester, **2**, was obtained as reddish brown [32,33].

2.2. Synthesis of 4-(1H-indol-3-yl)butanohydrazide (3)

4-(1*H*-indol-3-yl)butanoate (0.15 mol.; **2**) in 60 mL methanol and hydrazine monohydrate (80 %; 25 mL) was taken in a 500 mL round bottom flask. The reaction mixture was stirred for 14 h at room temperature (RT). After absolute conversion, the acid hydrazide was obtained by distilling methanol off from the reaction mixture. The precipitates were filtered, washed with cold *n*-hexane and air-dried to get pure 4-(1*H*-indol-3-yl)butanohydrazide (**3**) [32,33].

2.3. Synthesis of 5-[3-(1H-indol-3-yl)propyl]-4-phenyl-4H-1,2,4-triazole-3-thiol (5)

4-(1*H*-Indol-3-yl)butanohydrazide (0.13 mol.; 3) in absolute ethanol (30 mL) and KOH (0.13 mol) were taken in a round bottom flask. Phenyl isothiocyanate (4) was added subsequently. Mixture was refluxed for 16 h. On completion of the reaction, excess chilled distilled water and dil.

HCl was added to adjust pH 5–6. The precipitates were filtered, washed and dried to get desired cyclized product, **5** [31].

2.4. Preparation of 4-chloro-N-(substituted-phenyl)butanamides (8a-i)

Preparation of various 4-chloro-*N*-(substituted-phenyl)butanamides (**8a-i**) was carried out by reaction of various substituted anilines (**6a-i**) with 4-chlorobutanoyl chloride (**7**) in equimolar quantities (0.001 mol) and shaking manually in 10 % aqueous Na_2CO_3 solution. Solid precipitates were formed after 20–30 min, which were filtered and washed with cold distilled water to obtain the desired electrophiles, **8a-i**.

2.5. Synthesis of 4-({5-[3-(1H-indol-3-yl)propyl]-4-phenyl-4H-1,2,4-triazol-3-yl}sulfanyl)-N-(substituted-phenyl)butanamides (9a-i)

5-[3-(1*H*-Indol-3-yl)propyl]-4-phenyl-4*H*-1,2,4-triazole-3-thiol (0.2 g, **5**) was added in DMF (5 mL) contained in a 250 mL round bottom flask at room temperature, added one pinch of LiH and stirred for 30 min. Then different 4-chloro-*N*-(substituted-phenyl)butanamides **(8a-i)** were added in equimolar amounts separately in each respective reaction and stirred for 60–70 h. The completion of the reaction was monitored by TLC and after its completion; the reaction mixture was quenched with ice cold water (100 mL). The respective derivatives, **(9a-i)**, were collected through filtration or solvent extraction according to nature of the product.

2.5.1. 4-({5-[3-(1H-Indol-3-yl)propyl]-4-phenyl-4H-1,2,4-triazol-3-yl} sulfanyl)-N-(2-methylphenyl)butanamide (9a)

Light brown amorphous solid; Mol. formula $C_{30}H_{31}N_5SO$; Mol. mass 509 $gmol^{-1}$; yield: 74 %; melting point 186 °C; IR (KBr, cm^{-1}): υ 3217 (N—H str.), 3055 (C—H str. of aromatic ring), 2878 (C—H str. of aliphatic), 1583 (C═C aromatic str.), 1156 (C—N—C bond str.), 680 (C-S str.) cm^{-1}; ^{1}H NMR (600 MHz, DMSO-d_6, δ/ppm): δ 10.71 (s, 1H, NH-1), 9.28 (s, 1H, CONH), 7.54-7.51 (m, 3H, H-3′′, H-4′′ & H-5′′), 7.38-7.36 (m, 3H, H-7, H-2′′ & H-6′′), 7.31 (br.d, J = 8.1 Hz, 1H, H-4), 7.26 (br.d, J = 7.6 Hz, 1H, H-6′′′′), 7.22-7.18 (m, 1H, H-3′′′′), 7.13 (br.t, J = 7.5 Hz, 1H, H-5′′′′), 7.07 (br.t, J = 7.4 Hz, 1H, H-4′′′′), 7.04 (br.t, J = 7.3 Hz, 1H, H-6), 6.97 (br.s, 1H, H-2), 6.93 (br.t, J = 7.4 Hz, 1H, H-5), 3.12 (t, J = 6.9 Hz, 2H, CH_2-4′′′), 2.64 (t, J = 7.5 Hz, 2H, CH_2-3′), 2.58 (t, J = 7.4 Hz, 2H, CH_2-1′), 2.41 (t, J = 6.9 Hz, 2H, CH_2-2′′′), 2.08 (s, 3H, CH_3-2′′′′), 1.96 (q, J = 7.1 Hz, 2H, CH_2-3′′′), 1.88 (q, J = 7.3 Hz, 2H, CH_2-2′); ^{13}C NMR (150 MHz, DMSO-d_6, δ/ppm): δ 170.18 (C-1′′′), 155.48 (C-5′′), 149.49 (C-3′′), 138.05 (C-1′′′′), 136.23 (C-8), 135.23 (C-2′′′′), 133.18 (C-1′′), 129.84 (C-4′′), 129.78 (C-3′′ & C-5′′), 129.32 (C-3′′′′), 128.73 (C-6′′′′), 127.15 (C-2′′ & C-6′′), 127.02 (C-9), 126.47 (C-4′′′′), 125.79 (C-5′′′′), 122.20 (C-2), 120.76 (C-6), 118.19 (C-7), 118.07 (C-5), 113.52 (C-3), 111.25 (C-4), 34.35 (C-2′′′), 31.74 (C-4′′′), 26.93 (C-2′), 25.94 (C-3′′′), 24.36 (C-1′), 23.95 (C-3′), 17.57 (CH_3-2′′′′); Anal. Calc. for $C_{30}H_{31}N_5SO$ (509.22): C, 70.70; H, 6.13; N, 13.74. Found: C, 70.65; H, 6.07; N, 13.67. EI-MS (m/z): 509 $(C_{30}H_{31}N_5SO)^{+\cdot}$ $(M)^+$, 366 $(C_{20}H_{22}N_4SO)^+$, 334 $(C_{19}H_{18}N_4S)^{+\cdot}$, 190 $(C_9H_8N_3S)^+$, 175 $(C_{11}H_{13}NO)^+$, 159 $(C_{11}H_{13}N)^+$, 143 $(C_{10}H_9N)^+$, 130 $(C_9H_8N)^+$, 91 $(C_6H_5N)^+$, 77 $(C_6H_5)^+$.

2.5.2. 4-({5-[3-(1H-Indol-3-yl)propyl]-4-phenyl-4H-1,2,4-triazol-3-yl} sulfanyl)-N-(3-methylphenyl)butanamide (9b)

Light brown amorphous solid; Mol. formula $C_{30}H_{31}N_5SO$; Mol. mass 509 $gmol^{-1}$; yield: 74 %; melting point 206 °C; IR (KBr, cm^{-1}): υ 3217 (N—H str.), 3057 (C—H str. of aromatic ring), 2874 (C—H str. of aliphatic), 1583 (C═C aromatic str.), 1157 (C—N—C bond str.), 682 (C-S str.) cm^{-1}; ^{1}H NMR (600 MHz, DMSO-d_6, δ/ppm): δ 10.72 (s, 1H, NH-1), 9.46 (s, 1H, CONH), 7.54-7.49 (m, 3H, H-3′′, H-4′′ & H-5′′), 7.46 (br.s, 1H, H-2′′′′), 7.43 (br.d, J = 7.9 Hz, 1H, H-6′′′′), 7.37-7.35 (m, 3H, H-7, H-2′′ & H-6′′), 7.30 (br.d, J = 8.0 Hz, 1H, H-4), 7.23 (br.t, J = 7.8 Hz, 1H, H-5′′′′), 7.04 (br.t, J = 7.6 Hz, 1H, H-6), 6.97 (br.s, 1H, H-2), 6.94-6.91 (m, 2H, H-5 & H-4′′′′), 3.80 (t, J = 7.0 Hz, 2H, CH_2-4′′′), 2.63 (t, J = 7.4 Hz, 2H, CH_2-3′), 2.47 (t, J = 7.8 Hz, 4H, CH_2-1′ & CH_2-2′′′), 2.30 (s, 3H, CH_3-3′′′′), 2.05 (q, J = 7.5 Hz, 2H, CH_2-3′′′), 1.83 (q, J = 7.4 Hz, 2H, CH_2-2′); ^{13}C NMR (150 MHz, DMSO-d_6, δ/ppm): δ 167.58 (C-1′′′), 152.11 (C-5′′), 149.49 (C-3′′), 139.53 (C-1′′′′), 137.77 (C-3′′′′), 136.23 (C-8), 133.74 (C-1′′), 129.34 (C-4′′), 129.32 (C-3′′ & C-5′′), 128.37 (C-5′′′′), 128.14 (C-2′′ & C-6′′), 126.96 (C-9), 124.47 (C-4′′′′), 122.20 (C-2), 120.79 (C-6), 119.93 (C-2′′′′), 118.14 (C-7), 118.05 (C-5), 116.59 (C-6′′′′), 113.35 (C-3), 111.27 (C-4), 36.19 (C-2′′′), 32.31 (C-4′′′), 27.31 (C-2′), 25.94 (C-3′′′), 24.95 (C-1′), 23.79 (C-3′), 21.19 (CH_3-3′′′′); Anal. Calc. for $C_{30}H_{31}N_5SO$ (509.22): C, 70.70; H, 6.13; N, 13.74. Found: C, 70.65; H, 6.07; N, 13.67. EI-MS (m/z): 509 $(C_{30}H_{31}N_5SO)^{+\cdot}$ $(M)^+$, 366 $(C_{20}H_{22}N_4SO)^+$, 334 $(C_{19}H_{18}N_4S)^{+\cdot}$, 190 $(C_9H_8N_3S)^+$, 175 $(C_{11}H_{13}NO)^+$, 159 $(C_{11}H_{13}N)^+$, 143 $(C_{10}H_9N)^+$, 130 $(C_9H_8N)^+$, 91 $(C_6H_5N)^+$, 77 $(C_6H_5)^+$.

2.5.3. 4-({5-[3-(1H-Indol-3-yl)propyl]-4-phenyl-4H-1,2,4-triazol-3-yl} sulfanyl)-N-(4-methylphenyl)butanamide (9c)

Light brown amorphous solid; Mol. formula $C_{30}H_{31}N_5SO$; Mol. mass 509 $gmol^{-1}$; yield: 81 %; melting point 166 °C; IR (KBr, cm^{-1}): υ 3219 (N—H str.), 3055 (C—H str. of aromatic ring), 2874 (C—H str. of aliphatic), 1585 (C═C aromatic str.), 1156 (C—N—C bond str.), 681 (C-S str.) cm^{-1}; ^{1}H NMR (600 MHz, DMSO-d_6, δ/ppm): δ 10.73 (s, 1H, NH-1), 9.84 (s, 1H, CONH), 7.54-7.50 (m, 3H, H-3′′, H-4′′ & H-5′′), 7.48 (br.d, J = 8.4 Hz, 2H, H-2′′′′ & H-6′′′′), 7.39-7.35 (m, 3H, H-7, H-2′′ & H-6′′), 7.31 (br.d, J = 8.1 Hz, 1H, H-4), 7.06 (br.d, J = 8.2 Hz, 2H, H-3′′′′ & H-5′′′′), 7.04 (br.t, J = 7.7 Hz, 1H, H-6), 6.97 (dist.d, J = 1.6 Hz, 1H, H-2), 6.93 (br.t, J = 7.6 Hz, 1H, H-5), 3.10 (t, J = 7.2 Hz, 2H, CH_2-4′′′), 2.64 (t, J = 7.5 Hz, 2H, CH_2-3′), 2.57 (t, J = 7.5 Hz, 2H, CH_2-1′), 2.36 (t, J = 7.3 Hz, 2H, CH_2-2′′′), 2.08 (s, 3H, CH_3-4′′′′), 1.92 (q, J = 7.2 Hz, 2H, CH_2-3′′′), 1.88-1.85 (m, 2H, CH_2-2′); ^{13}C NMR (150 MHz, DMSO-d_6, δ/ppm): δ 169.99 (C-1′′′), 155.45 (C-5′′), 149.45 (C-3′′), 136.68 (C-1′′′′), 136.23 (C-8), 133.17 (C-1′′), 131.82 (C-4′′′′), 129.81 (C-4′′), 129.77 (C-3′′ & C-5′′), 128.95 (C-3′′′′ & C-5′′′′), 128.17 (C-2′′ & C-6′′), 127.02 (C-9), 122.18 (C-2), 120.76 (C-6), 119.04 (C-2′′′′ & C-6′′′′), 118.18 (C-7), 118.04 (C-5), 113.52 (C-3), 111.26 (C-4), 34.85 (C-2′′′), 31.72 (C-4′′′), 26.93 (C-2′), 25.97 (C-3′′′), 24.95 (C-1′), 24.36 (C-3′), 20.38 (CH_3-4′′′′); Anal. Calc. for $C_{30}H_{31}N_5SO$ (509.22): C, 70.70; H, 6.13; N, 13.74. Found: C, 70.65; H, 6.07; N, 13.67. EI-MS (m/z): 509 $(C_{30}H_{31}N_5SO)^{+\cdot}$ $(M)^+$, 366 $(C_{20}H_{22}N_4SO)^+$, 334 $(C_{19}H_{18}N_4S)^{+\cdot}$, 190 $(C_9H_8N_3S)^+$, 175 $(C_{11}H_{13}NO)^+$, 159 $(C_{11}H_{13}N)^+$, 143 $(C_{10}H_9N)^+$, 130 $(C_9H_8N)^+$, 91 $(C_6H_5N)^+$, 77 $(C_6H_5)^+$.

2.5.4. N-(4-Ethoxyphenyl)-4-({5-[3-(1H-indol-3-yl)propyl]-4-phenyl-4H-1,2,4-triazol-3-yl}sulfanyl)butanamide (9d)

Gray amorphous solid; Mol. formula $C_{31}H_{33}N_5SO_2$; Mol. mass 539 $gmol^{-1}$; yield: 89 %; melting point 187 °C; IR (KBr, cm^{-1}): υ 3185 (N—H str.), 3080 (C—H str. of aromatic ring), 2928 (C—H str. of aliphatic), 1587 (C═C aromatic str.), 1153 (C—N—C bond str.), 680 (C-S str.) cm^{-1}; ^{1}H NMR (600 MHz, DMSO-d_6, δ/ppm): δ 10.73 (s, 1H, NH-1), 9.77 (s, 1H, CONH), 7.56-7.51 (m, 3H, H-3′′, H-4′′ & H-5′′), 7.48 (br.dd, J = 3.0 & 8.4 Hz, 2H, H-2′′′′ & H-6′′′′), 7.39-7.37 (m, 3H, H-7, H-2′′ & H-6′′), 7.31 (br.d, J = 8.1 Hz, 1H, H-4), 7.04 (br.t, J = 7.2 Hz, 1H, H-6), 6.97 (dist.d, J = 1.6 Hz, 1H, H-2), 6.92 (br.t, J = 7.0 Hz, 1H, H-5), 6.84 (br.dd, J = 3.6 & 8.2 Hz, 2H, H-3′′′′ & H-5′′′′), 3.99 (quartet, J = 6.9 Hz, 2H, $CH_3\underline{CH_2}$O-4′′′′), 3.09 (t, J = 7.2 Hz, 2H, CH_2-4′′′), 2.65 (t, J = 7.5 Hz, 2H, CH_2-3′), 2.58 (t, J = 8.0 Hz, 2H, CH_2-1′), 2.44 (t, J = 7.3 Hz, 2H, CH_2-2′′′), 1.97 (q, J = 7.1 Hz, 2H, CH_2-3′′′), 1.89-1.87 (m, 2H, CH_2-2′), 1.31-1.28 (m, 3H, $\underline{CH_3}CH_2$O-4′′′′); ^{13}C NMR (150 MHz, DMSO-d_6, δ/ppm): δ 169.70 (C-1′′′), 155.49 (C-5′′), 154.90 (C-4′′′′), 149.45 (C-3′′), 136.23 (C-8), 133.17 (C-1′′), 132.27 (C-1′′′′), 129.81 (C-4′′), 129.77 (C-3′′ & C-5′′), 128.17 (C-2′′ & C-6′′), 127.01 (C-9), 122.20 (C-2), 120.79 (C-2′′′′ & C-6′′′′), 120.76 (C-6), 118.18 (C-7), 118.04 (C-5), 114.23 (C-3′′′′ & C-5′′′′), 113.52 (C-3), 111.26 (C-4), 63.06 ($CH_3\underline{CH_2}$O-4′′′′), 34.76 (C-2′′′), 31.72 (C-4′′′), 26.92 (C-2′), 25.96 (C-3′′′), 24.35 (C-1′), 23.95 (C-3′), 14.65 ($\underline{CH_3}CH_2$O-4′′′′); Anal. Calc. for $C_{31}H_{33}N_5SO_2$ (539.24): C, 68.99; H, 6.16; N, 12.98. Found: C, 68.91; H,

6.10; N, 12.92. EI-MS (*m/z*): 539 $(C_{31}H_{33}N_5SO_2)^{+\cdot}$ $(M)^+$, 396 $(C_{21}H_{24}N_4SO_2)^+$, 334 $(C_{19}H_{18}N_4S)^{+\cdot}$, 206 $(C_{12}H_{16}NO_2)^+$, 190 $(C_9H_8N_3S)^+$, 159 $(C_{11}H_{13}N)^+$, 143 $(C_{10}H_9N)^+$, 130 $(C_9H_8N)^+$, 91 $(C_6H_5N)^+$, 77 $(C_6H_5)^+$.

2.5.5. N-(2,3-Dimethylphenyl)-4-({5-[3-(1H-indol-3-yl)propyl]-4-phenyl-4H-1,2,4-triazol-3-yl}sulfanyl)butanamide (9e)

Brown sticky liquid; Mol. formula: $C_{31}H_{33}N_5SO$; Mol. Mass: 523 $gmol^{-1}$; yield: 78 %; IR (KBr, cm^{-1}): *υ* 3184 (N—H str.), 3080 (C—H str. of aromatic ring), 2926 (C—H str. of aliphatic), 1589 (C═C aromatic str.), 1151 (C—N—C bond str.), 684 (C-S str.) cm^{-1}; ^1H NMR (600 MHz, DMSO-*d*$_6$, *δ*/ppm): *δ* 10.72 (s, 1H, NH-1), 9.34 (s, 1H, CONH), 7.55-7.51 (m, 3H, H-3′′, H-4′′ & H-5′′), 7.44-7.43 (m, 1H, H-6′′′′), 7.38-7.35 (m, 3H, H-7, H-2′′ & H-6′′), 7.31 (br.d, *J* = 8.0 Hz, 1H, H-4), 7.05-7.01 (m, 3H, H-6, H-4′′′′ & H-5′′′′), 6.97 (br.s, 1H, H-2), 6.93 (br.t, *J* = 7.4 Hz, 1H, H-5), 3.12 (t, *J* = 7.1 Hz, 2H, CH_2-4′′′), 2.74 (t, *J* = 8.0 Hz, 2H, CH_2-2′′′), 2.68-2.64 (m, 2H, CH_2-3′), 2.58 (t, *J* = 7.4 Hz, 2H, CH_2-1′), 2.22 (s, 3H, CH_3-3′′′′), 2.08 (s, 3H, CH_3-2′′′′), 1.97-1.93 (m, 2H, CH_2-3′′′), 1.91-1.87 (m, 2H, CH_2-2′); ^{13}C NMR (150 MHz, DMSO-*d*$_6$, *δ*/ppm): *δ* 170.22 (C-1′′′), 155.48 (C-5′′), 149.49 (C-3′′), 136.75 (C-3′′′′), 136.23 (C-8), 136.10 (C-1′′′′), 133.99 (C-2′′′′), 133.19 (C-1′′), 129.83 (C-4′′′′), 129.78 (C-4′′), 129.76 (C-3′′ & C-5′′), 127.23 (C-5′′′′), 127.02 (C-9), 125.53 (C-2′′ & C-6′′), 122.21 (C-6′′′′), 122.18 (C-2), 120.77 (C-6), 118.18 (C-7), 118.04 (C-5), 113.53 (C-3), 111.26 (C-4), 36.29 (C-2′′′), 31.77 (C-4′′′), 26.94 (C-2′), 25.23 (C-3′′′), 24.36 (C-1′), 23.78 (C-3′), 20.09 (CH_3-3′′′′), 13.97 (CH_3-2′′′′); Anal. Calc. for $C_{31}H_{33}N_5SO$ (523.24): C, 71.10; H, 6.35; N, 13.37. Found: C, 71.01; H, 6.30; N, 13.29. EI-MS (*m/z*): 523 $(C_{31}H_{33}N_5SO)^{+\cdot}$ $(M)^+$, 380 $(C_{21}H_{24}N_4SO)^{+\cdot}$, 334 $(C_{19}H_{18}N_4S)^{+\cdot}$, 190 $(C_9H_8N_3S)^+$, 159 $(C_{11}H_{13}N)^+$, 143 $(C_{10}H_9N)^+$, 130 $(C_9H_8N)^+$, 91 $(C_6H_5N)^+$, 77 $(C_6H_5)^+$.

2.5.6. N-(2,4-Dimethylphenyl)-4-({5-[3-(1H-indol-3-yl)propyl]-4-phenyl-4H-1,2,4-triazol-3-yl}sulfanyl)butanamide (9f)

Brown sticky liquid; Mol. formula: $C_{31}H_{33}N_5SO$; Mol. Mass: 523 $gmol^{-1}$; yield: 78 %; IR (KBr, cm^{-1}): *υ* 3181 (N—H str.), 3078 (C—H str. of aromatic ring), 2926 (C—H str. of aliphatic), 1586 (C═C aromatic str.), 1150 (C—N—C bond str.), 684 (C-S str.) cm^{-1}; ^1H NMR (600 MHz, DMSO-*d*$_6$, *δ*/ppm): *δ* 10.72 (s, 1H, NH-1), 9.22 (s, 1H, CONH), 7.54-7.51 (m, 3H, H-3′′, H-4′′ & H-5′′), 7.38-7.36 (m, 3H, H-7, H-2′′ & H-6′′), 7.31 (br.d, *J* = 8.0 Hz, 1H, H-4), 7.20 (br.d, *J* = 7.9 Hz, 1H, H-6′′′′), 7.04 (br.t, *J* = 8.0 Hz, 1H, H-6), 6.98 (br.s, 1H, H-2′′′′), 6.97 (dist.d, *J* = 1.6 Hz, 1H, H-2), 6.94-6.92 (m, 2H, H-5 & H-5′′′′), 3.12 (t, *J* = 7.2 Hz, 2H, CH_2-4′′′), 2.66 (t, *J* = 7.4 Hz, 2H, CH_2-3′), 2.57 (t, *J* = 7.4 Hz, 2H, CH_2-1′), 2.41 (t, *J* = 7.3 Hz, 2H, CH_2-2′′′), 2.22 (s, 3H, CH_3-4′′′′), 2.11 (s, 3H, CH_3-2′′′′), 1.97 (q, *J* = 7.4 Hz, 2H, CH_2-3′′′), 1.87 (q, *J* = 7.3 Hz, 2H, CH_2-2′); ^{13}C NMR (150 MHz, DMSO-*d*$_6$, *δ*/ppm): *δ* 170.16 (C-1′′′), 155.49 (C-5′′), 149.51(C-3′′), 136.24 (C-8), 134.09 (C-1′′′′), 133.71 (C-2′′′′), 133.18 (C-1′′), 131.70 (C-4′′′′), 130.67 (C-3′′′′), 129.78 (C-3′′, C-4′′ & C-5′′), 127.22 (C-2′′ & C-6′′), 127.02 (C-9), 126.30 (C-5′′′′), 125.20 (C-6′′′′), 122.20 (C-2), 120.77 (C-6), 118.19 (C-7), 118.05 (C-5), 113.53 (C-3), 111.26 (C-4), 34.32 (C-2′′′), 31.76 (C-4′′′), 26.94 (C-2′), 25.52 (C-3′′′), 24.36 (C-1′), 23.95 (C-3′), 20.42 (CH_3-4′′′′), 17.74 (CH_3-2′′′′); Anal. Calc. for $C_{31}H_{33}N_5SO$ (523.24): C, 71.10; H, 6.35; N, 13.37. Found: C, 71.01; H, 6.30; N, 13.29. EI-MS (*m/z*): 523 $(C_{31}H_{33}N_5SO)^{+\cdot}$ $(M)^+$, 380 $(C_{21}H_{24}N_4SO)^{+\cdot}$, 334 $(C_{19}H_{18}N_4S)^{+\cdot}$, 190 $(C_9H_8N_3S)^+$, 159 $(C_{11}H_{13}N)^+$, 143 $(C_{10}H_9N)^+$, 130 $(C_9H_8N)^+$, 91 $(C_6H_5N)^+$, 77 $(C_6H_5)^+$.

2.5.7. N-(2,5-Dimethylphenyl)-4-({5-[3-(1H-indol-3-yl)propyl]-4-phenyl-4H-1,2,4-triazol-3-yl}sulfanyl)butanamide (9g)

White sticky liquid; Mol. formula: $C_{31}H_{33}N_5SO$; Mol. Mass: 523 $gmol^{-1}$; yield: 92 %; IR (KBr, cm^{-1}): *υ* 3224 (N—H str.), 3088 (C—H str. of aromatic ring), 2928 (C—H str. of aliphatic), 1585 (C═C aromatic str.), 1153 (C—N—C bond str.), 667 (C-S str.) cm^{-1}; ^1H NMR (600 MHz, DMSO-*d*$_6$, *δ*/ppm): *δ* 10.72 (s, 1H, NH-1), 9.23 (s, 1H, CONH), 7.55-7.51 (m, 3H, H-3′′, H-4′′ & H-5′′), 7.38-7.37 (m, 3H, H-7, H-2′′ & H-6′′), 7.31 (br.d, *J* = 8.1 Hz, 1H, H-4), 7.18 (br.s, 1H, H-6′′′′), 7.06-7.04 (m, 2H, H-6 & H-3′′′′), 6.97 (dist.d, *J* = 2.0 Hz, 1H, H-2), 6.93 (br.dt, *J* = 0.7 & 7.7 Hz, 1H, H-5), 6.87 (br.d, *J* = 7.5 Hz, 1H, H-4′′′′), 3.12 (t, *J* = 7.1 Hz, 2H, CH_2-4′′′), 2.65 (t, *J* = 7.4 Hz, 2H, CH_2-3′), 2.57 (t, *J* = 7.5 Hz, 2H, CH_2-1′), 2.42 (t, *J* = 7.2 Hz, 2H, CH_2-2′′′), 2.22 (s, 3H, CH_3-5′′′′), 2.11 (s, 3H, CH_3-2′′′′), 1.97 (q, *J* = 7.1 Hz, 2H, CH_2-3′′′), 1.89 (q, *J* = 7.3 Hz, 2H, CH_2-2′); ^{13}C NMR (150 MHz, DMSO-*d*$_6$, *δ*/ppm): *δ* 170.14 (C-1′′′), 155.49 (C-5′′), 149.51(C-3′′), 136.24 (C-8), 136.09 (C-1′′′′), 134.78 (C-5′′′′), 133.18 (C-1′′), 129.96 (C-3′′′′), 129.78 (C-3′′, C-4′′ & C-5′′), 128.54 (C-2′′′′), 127.23 (C-2′′ & C-6′′), 127.02 (C-9), 125.69 (C-4′′′′), 125.67 (C-6′′′′), 122.18 (C-2), 120.77 (C-6), 118.19 (C-7), 118.07 (C-5), 113.53 (C-3), 111.26 (C-4), 34.36 (C-2′′′), 31.74 (C-4′′′), 26.93 (C-2′), 25.24 (C-3′′′), 24.36 (C-1′), 23.95 (C-3′), 20.52 (CH_3-5′′′′), 17.40 (CH_3-2′′′′); Anal. Calc. for $C_{31}H_{33}N_5SO$ (523.24): C, 71.10; H, 6.35; N, 13.37. Found: C, 71.01; H, 6.30; N, 13.29. EI-MS (*m/z*): 523 $[M]^+$ $(C_{31}H_{33}N_5SO)^{+\cdot}$, 403 $C_{23}H_{24}N_4OS^+$, 380 $(C_{21}H_{24}N_4SO)^{+\cdot}$, 334 $(C_{19}H_{18}N_4S)^{+\cdot}$, 190 $(C_9H_8N_3S)^+$, 159 $(C_{11}H_{13}N)^+$, 143 $(C_{10}H_9N)^+$, 130 $(C_9H_8N)^+$, 91 $(C_6H_5N)^+$, 77 $(C_6H_5)^+$.

2.5.8. N-(2,6-Dimethylphenyl)-4-({5-[3-(1H-indol-3-yl)propyl]-4-phenyl-4H-1,2,4-triazol-3-yl}sulfanyl)butanamide (9h)

White amorphous solid; Mol. formula $C_{31}H_{33}N_5SO$; Mol. mass 523 $gmol^{-1}$; yield: 81 %; melting point 194 °C; IR (KBr, cm^{-1}): *υ* 3224 (N—H str.), 3088 (C—H str. of aromatic ring), 2928 (C—H str. of aliphatic), 1585 (C═C aromatic str.), 1153 (C—N—C bond str.), 667 (C-S str.) cm^{-1}; ^1H NMR (600 MHz, DMSO-*d*$_6$, *δ*/ppm): *δ* 10.72 (s, 1H, NH-1), 9.22 (s, 1H, CONH), 7.53-7.51 (m, 3H, H-3′′, H-4′′ & H-5′′), 7.37-7.35 (m, 3H, H-7, H-2′′ & H-6′′), 7.30 (br.d, *J* = 8.0 Hz, 1H, H-4), 7.15-7.09 (m, 3H, H-3′′′′, H-4′′′′ & H-5′′′′), 7.03 (br.t, *J* = 7.7 Hz, 1H, H-6), 6.97 (br.s, 1H, H-2), 6.92 (br.t, *J* = 7.5 Hz, 1H, H-5), 3.52 (t, *J* = 6.9 Hz, 2H, CH_2-4′′′), 2.64 (t, *J* = 7.4 Hz, 2H, CH_2-3′), 2.47 (t, *J* = 7.5 Hz, 2H, CH_2-1′), 2.41 (t, *J* = 7.9 Hz, 2H, CH_2-2′′′), 2.11 (s, 6H, CH_3-2′′′′ & CH_3-6′′′′), 2.15 (q, *J* = 7.5 Hz, 2H, CH_2-3′′′), 1.83 (q, *J* = 7.4 Hz, 2H, CH_2-2′); ^{13}C NMR (150 MHz, DMSO-*d*$_6$, *δ*/ppm): *δ* 169.82 (C-1′′′), 155.49 (C-5′′), 149.48 (C-3′′), 136.23 (C-1′′′′), 136.18 (C-8), 135.07 (C-2′′′′ & C-6′′′′), 133.18 (C-1′′), 129.80 (C-3′′ & C-5′′), 128.18 (C-4′′), 127.53 (C-3′′′′ & C-5′′′′), 127.24 (C-2′′ & C-6′′), 127.01 (C-9), 126.23 (C-4′′′′), 122.19 (C-2), 120.75 (C-6), 118.15 (C-7), 118.03 (C-5), 113.50 (C-3), 111.26 (C-4), 33.92 (C-2′′′), 31.80 (C-4′′′), 26.92 (C-2′), 25.37 (C-3′′′), 24.36 (C-1′), 23.94 (C-3′), 18.08 (CH_3-2′′′′ & CH_3-6′′′′); Anal. Calc. for $C_{31}H_{33}N_5SO$ (523.24): C, 71.10; H, 6.35; N, 13.37. Found: C, 71.01; H, 6.30; N, 13.29. EI-MS (*m/z*): 523 $(C_{31}H_{33}N_5SO)^{+\cdot}$ $(M)^+$, 380 $(C_{21}H_{24}N_4SO)^{+\cdot}$, 334 $(C_{19}H_{18}N_4S)^{+\cdot}$, 190 $(C_9H_8N_3S)^+$, 159 $(C_{11}H_{13}N)^+$, 143 $(C_{10}H_9N)^+$, 130 $(C_9H_8N)^+$, 91 $(C_6H_5N)^+$, 77 $(C_6H_5)^+$.

2.5.9. N-(3,4-Dimethylphenyl)-4-({5-[3-(1H-indol-3-yl)propyl]-4-phenyl-4H-1,2,4-triazol-3-yl}sulfanyl)butanamide (9i)

Light brown amorphous solid; Mol. formula $C_{31}H_{33}N_5SO$; Mol. mass 523 $gmol^{-1}$; yield: 91 %; melting point 156 °C; IR (KBr, cm^{-1}): *υ* 3226 (N—H str.), 3089 (C—H str. of aromatic ring), 2928 (C—H str. of aliphatic), 1585 (C═C aromatic str.), 1150 (C—N—C bond str.), 667 (C-S str.) cm^{-1}; ^1H NMR (600 MHz, DMSO-*d*$_6$, *δ*/ppm): *δ* 10.72 (s, 1H, NH-1), 9.75 (s, 1H, CONH), 7.54-7.51 (m, 3H, H-3′′, H-4′′ & H-5′′), 7.38-7.33 (m, 4H, H-7, H-2′′, H-6′′ & H-2′′′′), 7.31-7.28 (m, 2H, H-4 & H-6′′′′), 7.05-7.02 (m, 2H, H-6 & H-5′′′′), 6.97 (dist.d, *J* = 2.1 Hz, 1H, H-2), 6.92 (br.dt, *J* = 0.9 & 7.8 Hz, 1H, H-5), 3.09 (t, *J* = 7.2 Hz, 2H, CH_2-4′′′), 2.65 (t, *J* = 7.4 Hz, 2H, CH_2-3′), 2.58 (t, *J* = 7.5 Hz, 2H, CH_2-1′), 2.37 (t, *J* = 7.3 Hz, 2H, CH_2-2′′′), 2.14 (s, 3H, CH_3-4′′′′), 2.08 (s, 3H, CH_3-3′′′′), 1.92 (q, *J* = 7.4 Hz, 2H, CH_2-3′′′), 1.86 (q, *J* = 7.5 Hz, 2H, CH_2-2′); ^{13}C NMR (150 MHz, DMSO-*d*$_6$, *δ*/ppm): *δ* 169.93 (C-1′′′), 155.48 (C-5′′), 149.45 (C-3′′), 136.99 (C-3′′′′), 136.23 (C-8), 136.09 (C-1′′′′), 133.18 (C-1′′), 130.61 (C-4′′′′), 129.83 (C-4′′), 129.77 (C-3′′ & C-5′′), 127.23 (C-2′′ & C-6′′), 127.02 (C-9), 125.53 (C-5′′′′), 122.18 (C-2), 120.76 (C-6), 120.32 (C-2′′′′), 118.19 (C-7), 118.04 (C-5), 116.61 (C-6′′′′), 113.52 (C-3), 111.25 (C-4), 34.85 (C-2′′′), 31.71 (C-4′′′), 26.93 (C-2′), 24.98 (C-3′′′), 24.36 (C-1′), 23.95 (C-3′), 19.57 (CH_3-3′′′′), 18.71 (CH_3-4′′′′); Anal. Calc. for $C_{31}H_{33}N_5SO$ (523.24): C, 71.10; H,

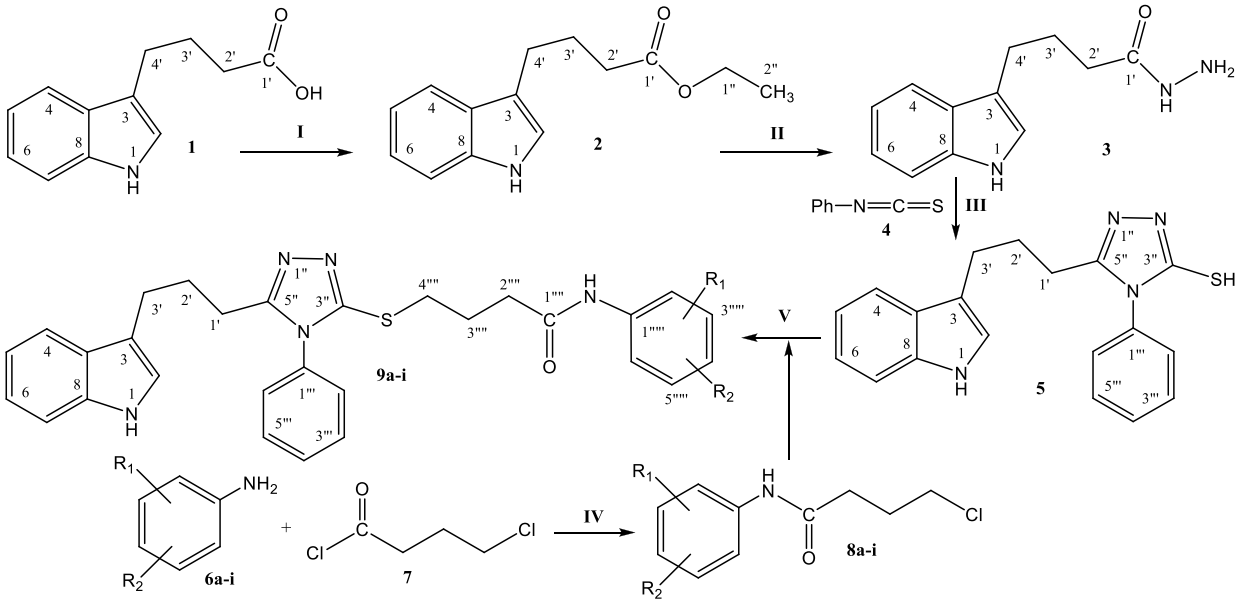

6a, 8a, 9a : R^1 = H; R^2 = 2-CH_3 **6c, 8c, 9c** : R^1 = H; R^2 = 4-CH_3 **6e, 8e, 9e** : R^1 = 2-CH_3; R^2 = 3-CH_3 **6g, 8g, 9g** : R^1 = 2-CH_3; R^2 = 5-CH_3
6b, 8b, 9b : R^1 = H; R^2 = 3-CH_3 **6d, 8d, 9d** : R^1 = H; R^2 = 4-OC_2H_5 **6f, 8f, 9f** : R^1 = 2-CH_3; R^2 = 4-CH_3 **6h, 8h, 9h** : R^1 = 2-CH_3; R^2 = 6-CH_3
6i, 8i, 9i : R^1 = 3-CH_3; R^2 = 4-CH_3

Scheme 1. Outline for the synthesis of 4-({5-[3-(1*H*-indol-3-yl)propyl]-4-phenyl-4*H*-1,2,4-triazol-3-yl}-sulfanyl)-*N*-(substituted-phenyl)butanamides (**9a-i**). Reagents & Conditions: (I) EtOH/H_2SO_4/refluxing for 8 h. (II) MeOH/N_2H_4•H_2O/refluxing for 14 h. (III) MeOH/**4**/Refluxing for 16 h/ppt. dissolved in 10 % NaOH/filtration/acidification of filtrate in cold state. (IV) Aq. Na_2CO_3 soln./pH 9–10/vigorous shaking at RT for 20–30 min. (V) DMF/LiH/stirring for 60–70 h.

6.35; N, 13.37. Found: C, 71.01; H, 6.30; N, 13.29. EI-MS (*m/z*): 523 $(C_{31}H_{33}N_5SO)^{+\cdot}$ $(M)^+$, 380 $(C_{21}H_{24}N_4SO)^{+\cdot}$, 334 $(C_{19}H_{18}N_4S)^{+\cdot}$, 190 $(C_9H_8N_3S)^+$, 159 $(C_{11}H_{13}N)^+$, 143 $(C_{10}H_9N)^+$, 130 $(C_9H_8N)^+$, 91 $(C_6H_5N)^+$, 77 $(C_6H_5)^+$.

2.6. In vitro alkaline phosphatase inhibition assay

Activity of calf intestinal alkaline phosphatase (CIALP) was measured by spectrophotometric assay as previously described by [34,35]. The reaction mixture comprised of 50 mM Tris–HCl buffer (5 mM $MgCl_2$, 0.1 mM $ZnCl_2$ pH 9.5), the compound (0.1 mM with final DMSO 1 % (v/v) and mixture was pre-incubated for 10 min by adding 5 μL of CIALP (0.025 U/mL). Then, 10 μL of substrate (0.5 mM *p*-NPP (para nitrophenyl phosphate disodium salt) was added to initiate the reaction and the assay mixture was incubated again for 30 min at 37 °C. The change in absorbance of released *p*-nitrophenolate was monitored at 405 nm, using a 96-well microplate reader (SpectraMax ABS, USA). All the experiments were repeated three times in a triplicate manner. KH_2PO_4 was used as the reference inhibitor of CIALP.

The Alkaline Phosphatase activities were calculated according to the following formula:

$$\text{Alkaline Phosphate Inhibition } (\%) = \left[\frac{(OD(control) - OD(sample)}{OD(control)}\right] \times 100$$

Where $OD_{control}$ and OD_{sample} represents the optical densities in the absence and presence of sample, respectively.

2.7. Kinetic mechanism analysis for ALP

Based on the IC_{50} results we select the most potent inhibitor **9h** for ALP to determine the mechanism of enzyme inhibition by following our reported method [36]. The inhibitor (**9h**) concentrations were used 0.00, 0.031, 0.062 and 0.124 μM. Substrate *p*-NPP concentrations were 10, 5, 2.5, 1.25, and 0.625 mM pre-incubation time and other conditions were same as described in alkaline phosphatase inhibition assay section. Maximal initial velocities were determined from initial linear portion of absorbances up to 10 min after addition of enzyme at per minute's interval. The inhibition type on the enzyme was assayed by Lineweaver-Burk plot of inverse of velocities (1/V) versus inverse of substrate concentration 1/[S] mM^{-1}. The EI dissociation constant K_i was determined by secondary plot of 1/V versus inhibitor concentration.

2.8. Hemolytic activity

Bovine blood samples were collected in EDTA that was diluted with saline (0.9 % NaCl), and centrifuge at 1000x*g* for 10 min. The erythrocytes separated diluted in phosphate buffer saline of pH 7.4 and a suspension was made. Add 20 μL of synthetic compounds solution (10 mg/mL) in 180 μL of RBCs suspension and incubate for 30 min at room temperature. PBS was used as negative control and Triton 100-X was taken as positive control [37,38]. The %age of hemolysis was taken as by using formula:

$$(\%)\ of\ Hemolysis = \frac{Absorbance\ of\ Sample - Absorbance\ of\ Negative\ Control}{Absorbance\ of\ Positive\ Control} \times 100$$

2.9. In silico computational methodology

The compounds were docked to crystal structure of human PLAP (PDB ID: 1ZED, resolution 1.57 Å) [39] which was obtained from the Protein Data Bank (PDB) [40,41]. The Scigress version FJ 2.6 program [42] was used to prepare the crystal structure for docking, i.e., hydrogen atoms were added, the co-crystallized ligand p-nitrophenyl-phosphonate (PNP)was removed as well as crystallographic water molecules. The docking centre for the binding pocket was defined as the position of the phenyl carbon bonded to the nitrogen atom in the PNP (x = 55.832, y = 28.945, z = −3.902) with 10 Å radius Fifty docking runs were allowed for each ligand with default search efficiency

Table 1
Alkaline phosphate enzyme inhibitory and hemolytic activity of bi-heterocyclic butanamides (**9a-i**).

Compounds	Aryl part	Alkaline phosphatase activity IC_{50} ± SEM (μM)	Hemolysis (%) (Mean ± SEM)
9a	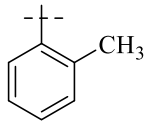	1.103 ± 0.524	12.77 ± 0.45
9b	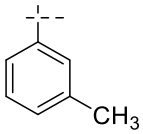	0.157 ± 0.098	15.40 ± 0.13
9c	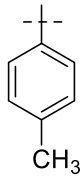	0.508 ± 0.127	12.40 ± 0.42
9d	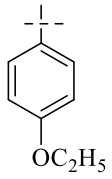	1.354 ± 0.663	14.00 ± 0.23
9e	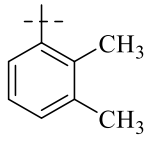	11.154 ± 0.923	13.77 ± 0.85
9f	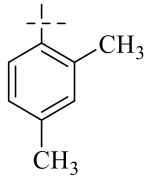	5.874 ± 0.376	17.00 ± 0.35
9g	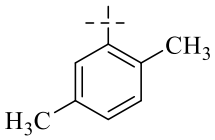	3.558 ± 0.211	17.22 ± 0.26
9h	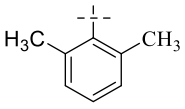	0.062 ± 0.017	10.33 ± 0.25
9i	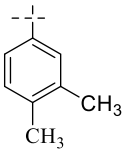	0.098 ± 0.052	20.00 ± 0.19
KH_2PO_4		**5.251 ± 0.468**	–
Triton X		–	45.32 ± 0.01

Note: SEM= Standard error of the mean; values are expressed in mean ± SEM. PBS Hemolysis = 2.45 ± 0.34 %.

(100 %). The basic amino acids lysine and arginine were defined as protonated. Furthermore, aspartic and glutamic acids were assumed to be deprotonated. The GoldScore (GS) [43] and ChemScore (CS) [44,45], ChemPLP (Piecewise Linear Potential) [46] and ASP (Astex Statistical Potential) [47] scoring functions were implemented to validate the predicted binding modes and relative energies of the ligands using the GOLD v5.4.1 software suite. The QikProp 3.2 [48] software package was used to calculate the molecular descriptors of the molecules. The reliability of it is established for the calculated descriptors [49].

2.10. Statistical analysis

All the measurements were carried out in triplicate and statistical); Analysis was performed by Microsoft Excel 2010. The results are presented as mean ± SEM with 96 % CL.

3. Results and discussions

In the presented research work, different derivatives of 5-[3-(1*H*-indol-3-yl)propyl]-4-phenyl-4*H*-1,2,4-triazol-3-yl sulfides were synthesized according to the outline illustrated in Scheme 1; Table 1. First, the, 4-(1*H*-indol-3-yl)butanoic acid (**1**) was subjected to esterification by ethanol in the presence of concentrated sulfuric acid taken in catalytic amount. The ethanol is used as reactant and also solvent in order to push the equilibrium towards product side, as it is a reversible reaction. The product was collected by solvent extraction after addition of a weak base and excess of water. The addition of base neutralized the unreacted carboxylic acid and the catalytic sulfuric acid. The salts of these acids were transferred to the aqueous layer while the resulting ester was partitioned to the organic phase during solvent extraction. Thus, ethyl 4-(1*H*-indol-3-yl)butanoate (**2**) was obtained as brownish liquid (amorphous solid at refrigeration). The second step was performed to convert **2** into respective carbohydrazide **3** by the nucleophillic hydrazine in the presence of an organic solvent like methanol or ethanol and stirring for 14 h at room temperature. This nucleophillic substitution reaction is generally carried out at room temperature but sometimes a little bit higher temperature in the form of reflux might be required. The completion of this reaction yielded 4-(1*H*-indol-3-yl)butanohydrazide (**3**) as light brown amorphous solid. The third step was a cyclization to form a heterocyclic ring through reaction with phenyl isothiocyanate (**4**). The resulting product was 5-[3-(1*H*-indol-3-yl)propyl]-4-phenyl-4*H*-1,2,4-triazole-3-thiol (**5**) having a mercapto group at its third carbon. Then, in last step, the acidic proton of this mercapto group was replaced with different 4-chloro-*N*-(substituted-phenyl)butanamides **(8a-i)** groups by reaction with different anilines, **8a-i**, in the presence of LiH using aprotic polar medium to get required derivatives (**9a-i**).

3.1. Chemistry

The structural analysis of one of the compounds is discussed here in detail for the articulacy of the reader. The molecule **9g** was obtained as a white amorphous solid. Its molecular formula, $C_{31}H_{33}N_5SO$, was established by CHN analysis data and its molecular ion peak at *m/z* 523 in its EI-MS spectrum (Fig. S1). The number of proton and carbon resonances in its ^{1H}NMR and ^{13C}NMR spectra were also in agreement with its deduced molecular formula. Different functionalities in this molecule were depicted by absorption bands in its IR spectrum (KBr, cm^{-1}): at *υ* 3224 (N—H str.), 3088 (C—H str. of aromatic ring), 2928 (C—H str. of aliphatic), 1585 (C═C aromatic str.), 1153 (C—N—C bond str.), 667 (C-S str.) cm^{-1}. With the help of ^{1H}NMR spectrum of this molecule, the indole heterocyclic core was identified clearly by the characteristic signals at *δ* 10.72 (s, 1H, NH-1), 7.38-7.37 (m, 3H, H-7, H-2′′ & H-6′′), 7.31 (br.d, *J* = 8.1 Hz, 1H, H-4), 7.06-7.04 (m, 2H, H-6 & H-3′′′′′), 6.97

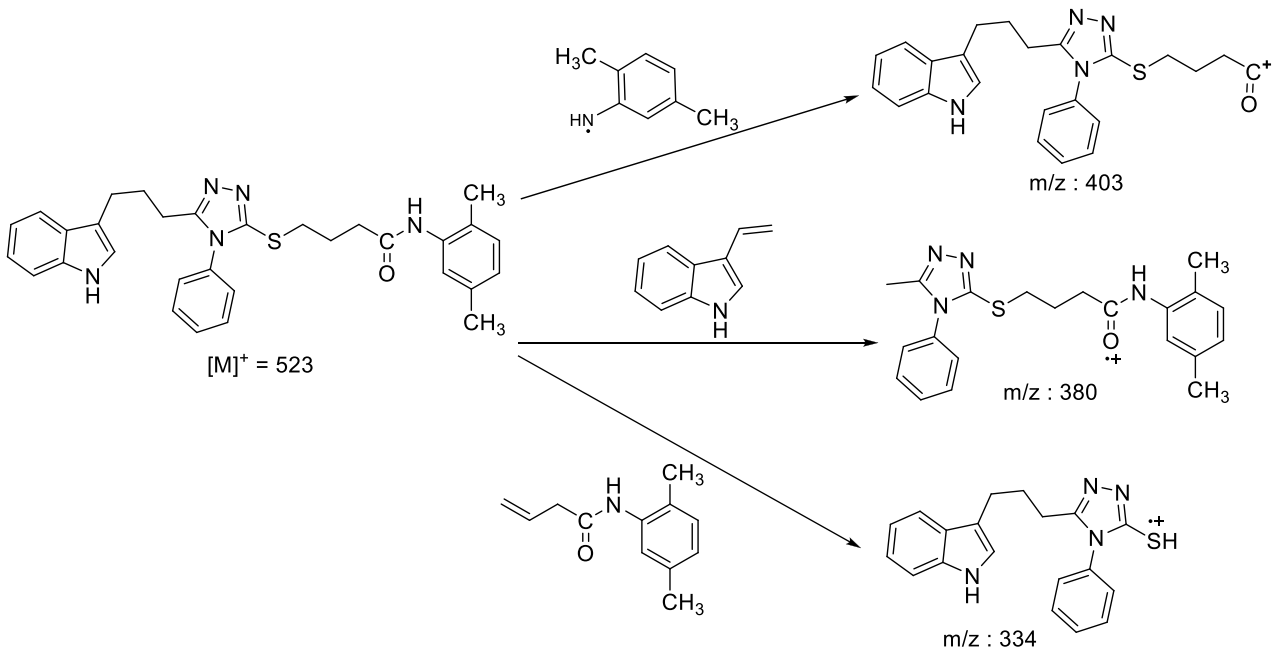

Fig. 2. EI-MS key fragmentation pattern of compound **9g**.

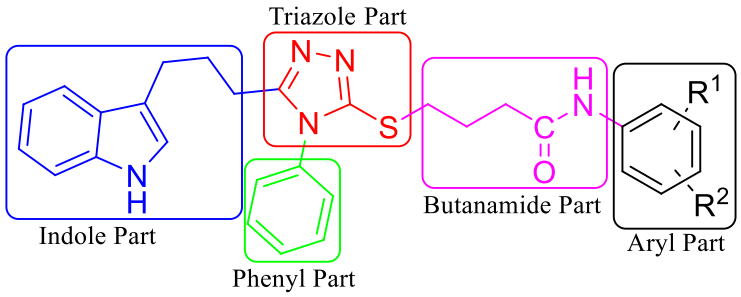

Fig. 3. General structural parts of compounds, **9(a-i)**.

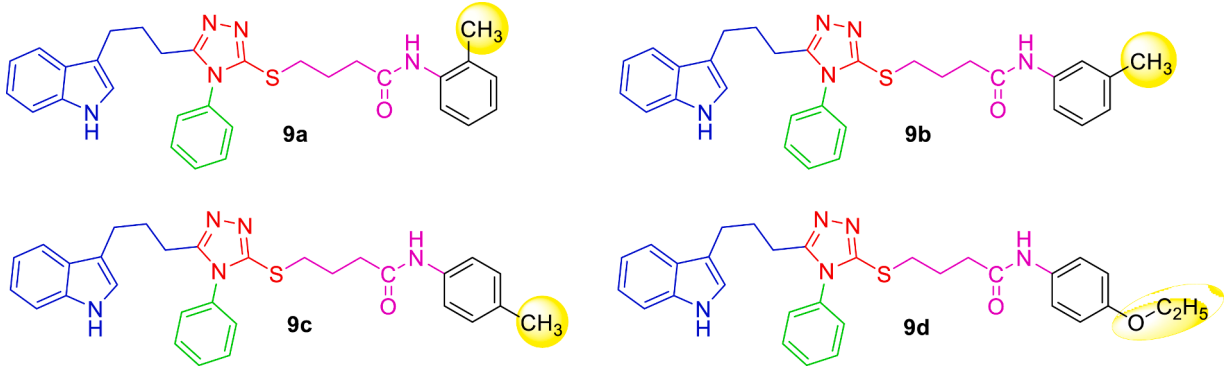

Fig. 4. SAR of compounds **9a, 9b, 9c** and **9d**.

(dist.d, $J = 2.0$ Hz, 1H, H-2), 6.93 (br.dt, $J = 0.7$ & 7.7 Hz, 1H, H-5). The phenyl ring attached at 1-postion of 1,2,4-triazole was characterized by two resonances at δ 7.55-7.51 (m, 3H, H-3′′, H-4′′ & H-5′′) and 7.38-7.37 (m, 3H, H-7, H-2′′ & H-6′′). Similarly, the resonances at δ 7.18 (br.s, 1H, H-6′′′′), 7.06-7.04 (m, 2H, H-6 & H-3′′′′), 6.87 (br.d, $J = 7.5$ Hz, 1H, H-4′′′′), 2.22 (s, 3H, CH_3-5′′′′) and 2.11 (s, 3H, CH_3-2′′′′) ppm, were typical for a 2,5-dimethylphenyl group substituted at nitrogen atom in the molecule. The *C* and *N*-substituted butanamido group was recognized by two signals at δ 9.23 (s, 1H, CONH), 3.12 (t, $J = 7.1$ Hz, 2H, CH_2-4′′′), 2.42 (t, $J = 7.2$ Hz, 2H, CH_2-2′′′) and 1.97 (q, $J = 7.1$ Hz, 2H, CH_2-3′′′). In the up-field region of spectrum, the signals of three intervening methylene groups at δ 2.65 (t, $J = 7.4$ Hz, 2H, CH_2-3′), 2.57 (t, $J = 7.5$ Hz, 2H, CH_2-1′) and 1.89 (q, $J = 7.3$ Hz, 2H, CH_2-2′), were helpful to ascertain the connectivity of indole moiety from its 3-position to the 5-position of 1,2,4-triazole scaffold. The ^{1}HNMR spectrum of this compound has been shown in Fig. S2a while Fig. S2b displayed the expanded aromatic region. The expanded aliphatic part of this spectrum has been shown in Fig. S2c.

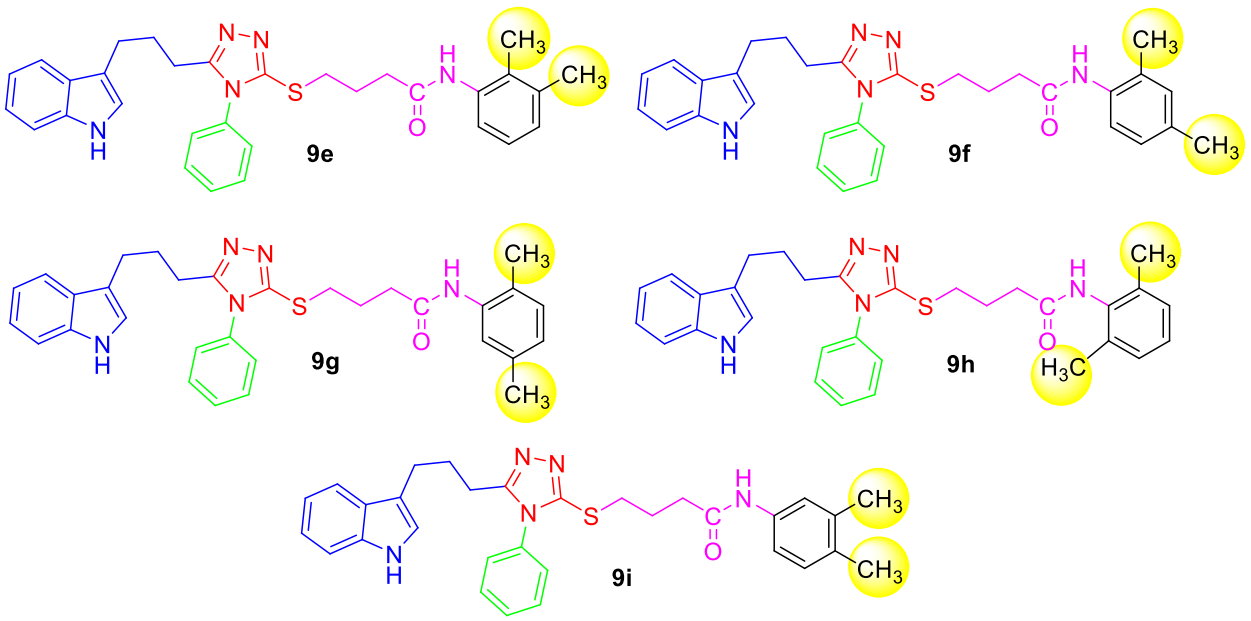

Fig. 5. SAR of compounds **9e, 9f, 9g, 9h** and **9i**.

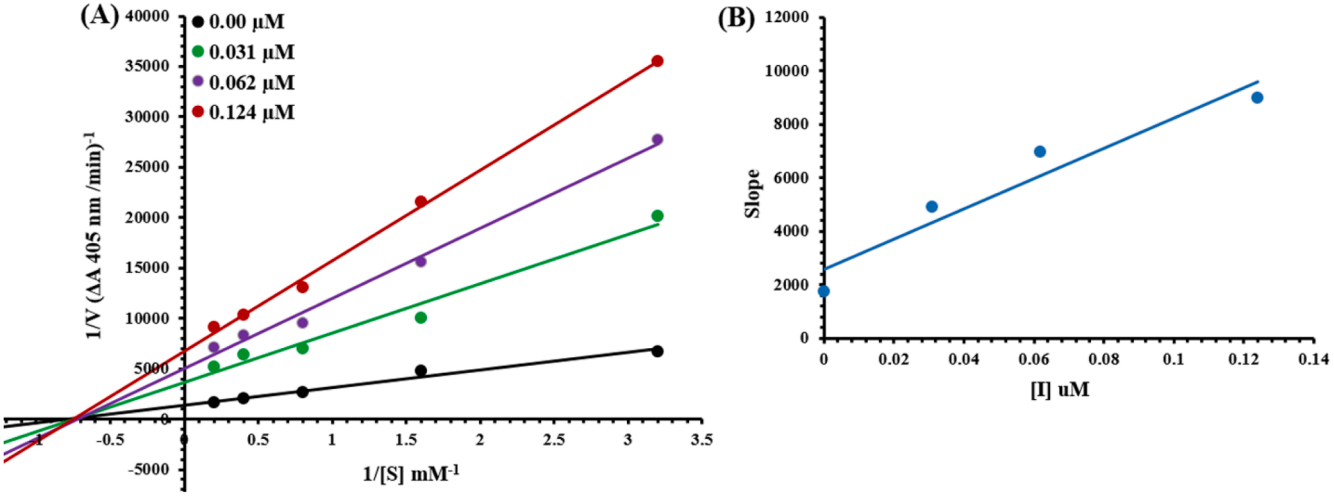

Fig. 6. Lineweaver–Burk plots for the inhibition of alkaline phosphatase in the presence of Compounds **9h**. (Fig. 6A). The insets represent the plot of the slope versus inhibitor concentrations to determine inhibition constant (Fig. 6B). The lines were drawn using linear least squares fit.

Table 2
Kinetic parameters of the alkaline phosphatase for para nitrophenyl phosphate disodium salt activity in the presence of different concentrations of **9h**.

Concentration (µM)	V_{max} (ΔA /Min)	K_m (mM)	Inhibition type	K_i (µM)
0.00	0.00063	1.2	Non-Competitive	0.045
0.031	0.00019	1.2		
0.062	0.00014	1.2		
0.124	0.00011	1.2		

V_{max} = the reaction velocity; K_m = Michaelis-Menten constant; K_i = EI dissociation constant.

The carbon skeleton of this molecule was also fully supported by its ^{13C}NMR spectrum, shown in the Fig. S3. The ^{13C}NMR spectrum depicted the signals of all the sixteen carbons, where the most downfield quaternary carbons signals at δ 155.49 (C-5′′) and 149.51 (C-2′′) belonged to the cyclized 1,2,4-triazole ring, thus confirming the formation of this ring. The other three quaternary carbons appearing at δ 136.24 (C-8), 127.02 (C-9) and 113.53 (C-3) ppm, were attribute of the indole core. The methine carbon resonances appearing at δ 122.18 (C-2), 120.77 (C-6), 118.19 (C-7), 118.07 (C-5), 111.26 (C-4) were also coherent with the indole moiety. The phenyl group substituted at nitrogen atom of 1,2,4-triazole was ascertained by one quaternary carbon signal at δ 133.18 (3′′′) and two methine carbon resonances at δ 129.78 (C-3′′′, C-4′′′ & C-5′′′) and 127.23 (C-2′′′ & C-6′′′). The *C* and *N*-substituted butanamido group was rational by four discrete resonances, one for a carbonyl group at δ 170.14 (C-1′′′′) and three methylene group at δ 34.36 (C-2′′′′), 31.74 (C-4′′′′) and 25.24 (C-3′′′′).The 2,5-di-methylphenyl group substituted at the nitrogen atom was demonstrated by eight signals at δ 136.09 (C-1′′′′′), 134.78 (C-5′′′′′), 129.96 (C-3′′′′′), 128.54 (C-2′′′′′), 125.69 (C-4′′′′′), 125.67 (C-6′′′′′), 20.52 (CH_3-5′′′′′), 17.40 (CH_3-2′′′′′) while three methylene signals appearing in up-field region at δ 26.93 (C-2′), 24.36 (C-1′) and 23.95 (C-3′), were assignable to those methylene groups, which were connecting the indole and triazole moieties together. So, on the basis of aforesaid cumulative evidences, the structure of **9g** was

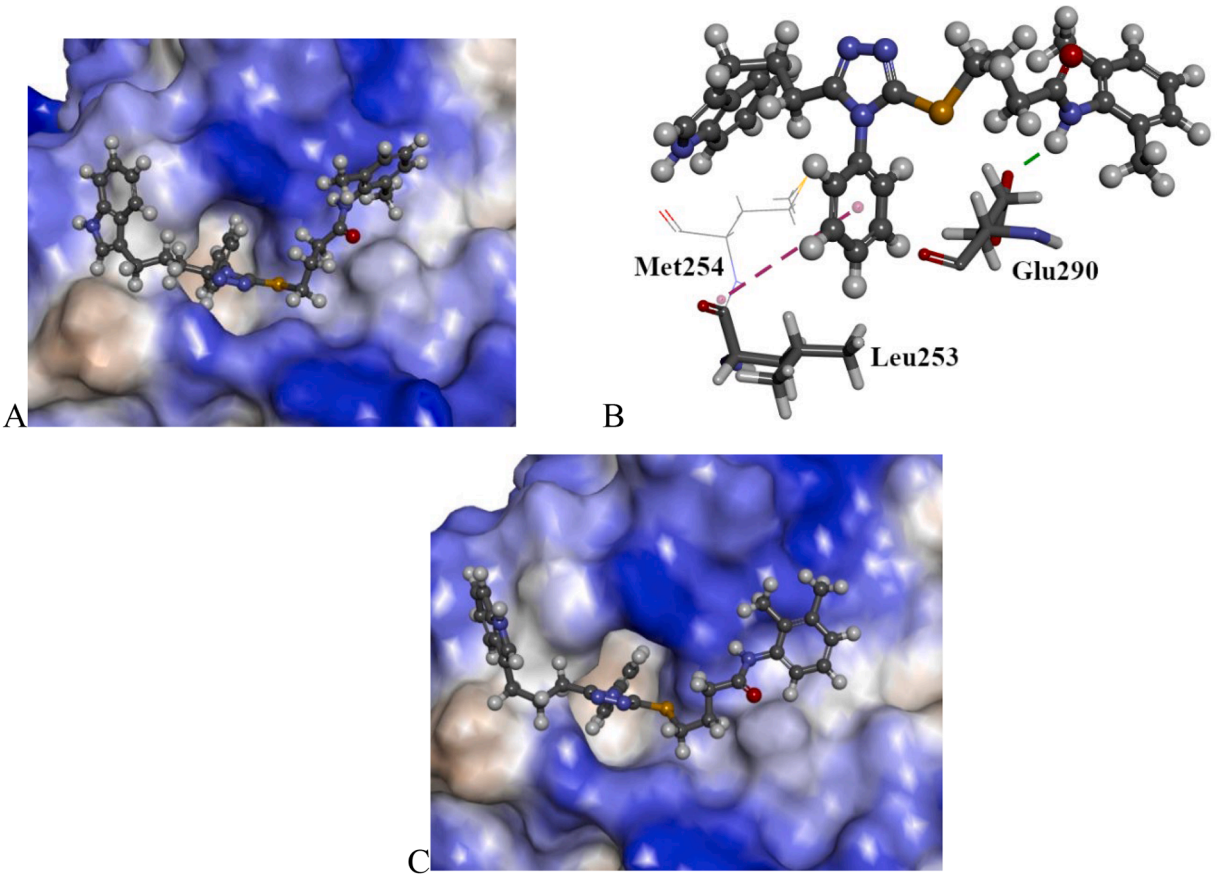

Fig. 7. The docked configuration of **9h**(A) and **9e**(C) in the peripheral site of PLAP.The protein surface is rendered. The ligand occupies the binding pocket. Blue depicts hydrophilic region on the surface, brown depicts hydrophobic region and gray shows neutral region. (B) Hydrogen bonds are shown as green lines between **9h** and the amino acids Glu290. ##### stack is form between **9h** and Leu253 for ChemScore configuration.

confirmed and it was named as *N*-(2,5-dimethylphenyl)-4-({5-[3-(1*H*-indol-3-yl)propyl]-4-phenyl-4*H*-1,2,4-triazol-3-yl}sulfanyl)butanamide (**9g**). A similar protocol was exercised for the structural characterization (Fig. S4-S19) of other derivatives in the synthesized series.

3.2. Mass spectrometry

The molecular ion peak of the parent molecule was observed at *m/z* 523 (Fig. 2), which was further cleaved in following ways (Fig. 2):

(A) The molecular ion *m/z* 523 was cleaved at peptide bond between carbonyl and amine group and resulted in formation of a cation $C_{23}H_{24}N_4OS^+$ at *m/z* 403.
(B) A radical cation $C_{21}H_{23}N_4OS^{+\cdot}$ at *m/z* 380 was seen by the cleavage of C—C sigma bond between carbon of indole chain and triazole ring, with the loss of a neutral fragment.
(C) Molecular cation at *m/z* 523 was also fragmentized between sulfur and butanamido chain to yield another radical cation $C_{19}H_{17}N_4S^{+\cdot}$ at *m/z* 334.

3.3. Alkaline phosphatase inhibition and structure-activity relationship

The synthesized di-heterocyclic multi-functional compounds, **9(a-i)** were tested against alkaline phosphate enzyme and their inhibitory potentials are tabulated in Table 1. These scaffolds exposed very excellent activities, as evident from their lower IC_{50} (μM) values, relative to standard, KH_2PO_4, having IC_{50} value of 5.251 ± 0.468 μM. Though the displayed activity is integrated for the whole molecule, yet a limited structure-activity relationship (SAR) was rational by inspecting the effect of varying heterocyclic entity on the inhibitory potential. Except this varying heterocyclic moiety, other parts in all molecules were same. The general structural units of the examined compounds are labeled in Fig. 3.

When the inhibitory potential of *ortho*-, *meta*- and *para*-substituted molecules was compared, it was revealed that **9b** (IC_{50} = 0.157 ± 0.098 μM) group was more prone to the inhibition of alkaline phosphate as compared it with *para*-substituted compound **9c** (IC_{50} = 0.508 ± 0.127 μM), *ortho*-substituted compound **9a** (IC_{50} = 1.103 ± 0.524 μM) and *para*-substituted ethoxy group compound **9d** (IC_{50} = 1.354 ± 0.663 μM) (Fig. 4). It means that the presence of smaller groups at *meta*-position can favor the inhibitory activity in these molecules.

Among the following three di-methylated regio-isomers, compound **9h** in which the two methyl groups were present on symmetry positions (2,6-dimethylphenyl) exhibited least inhibitory activity (IC_{50} = 0.062 ± 0.017 μM) as compared to other compounds **9e** (IC_{50} = 11.154 ± 0.923 μM), **9f** (IC_{50} = 5.874 ± 0.376 μM), **9g** (IC_{50} = 3.558 ± 0.211 μM) and **9i** (IC_{50} = 0.098 ± 0.052 μM). Even it was even least active in the whole series, yet it was much better inhibitor than standard, KH_2PO_4 (IC_{50} = 5.251 ± 0.468 μM). The results indicating that separation of the methyl groups probably augmented the suitable interactions with the active site of the enzyme (Fig. 5).

3.4. Kinetic mechanism for ALP

Presently most potent compound **9h** was studied for their mode of inhibition against alkaline phosphatase. The potential of the compounds to inhibit the free enzyme and enzyme-substrate complex was determined in terms of EI and ESI constants respectively. The kinetic studies

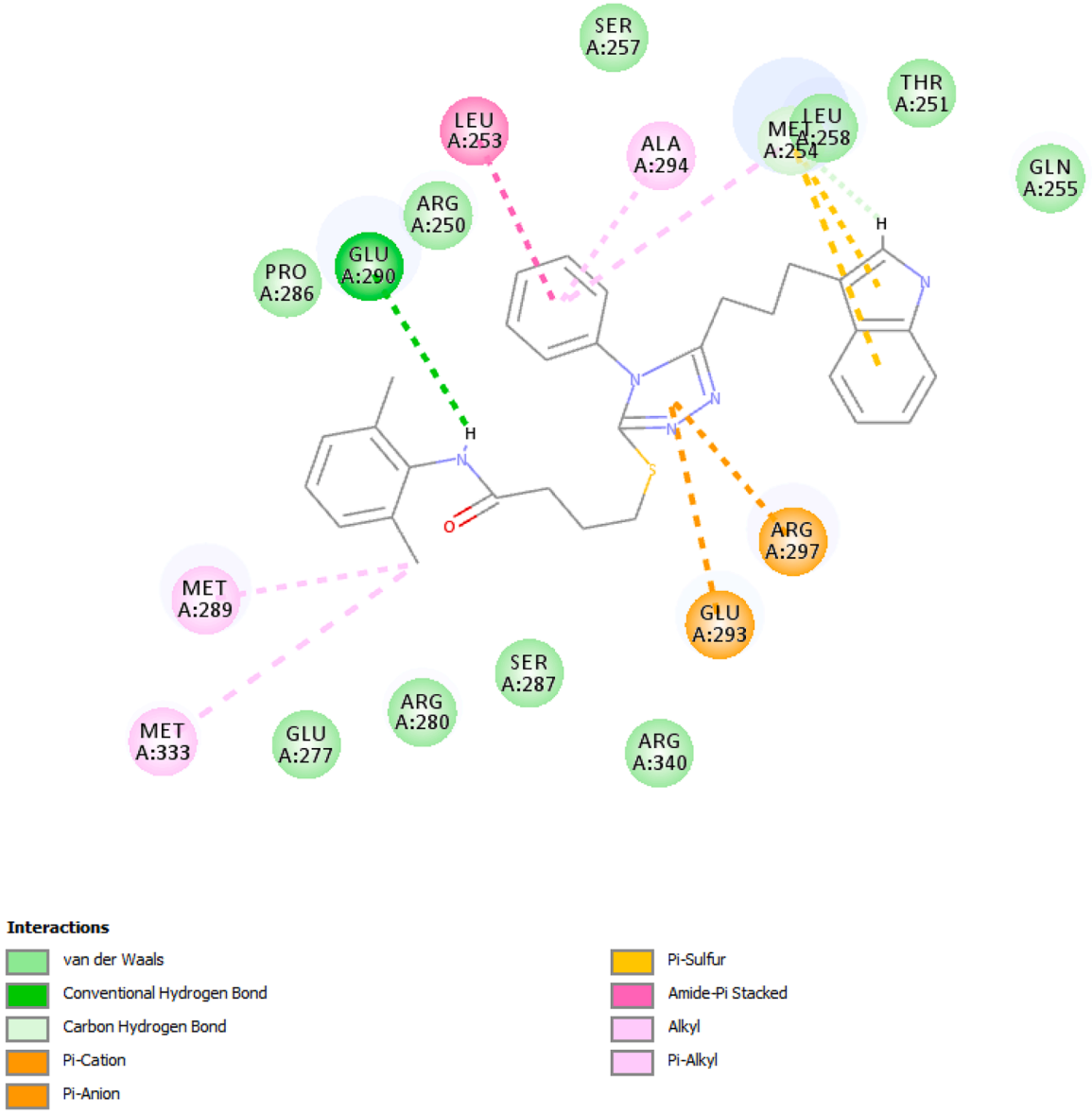

Fig. 8. The 2D representation of the interactions of **9h** with PLAP at the peripheral binding site.

Table 3
Results of the scoring function for the ligands, **9a-i**.

Ligand	ASP	ChemPLP	ChemScore	GoldScore
9a	33.0	79.4	26.8	62.2
9b	32.7	83.2	25.8	65.4
9c	33.2	81.5	28.0	65.0
9d	34.3	82.5	26.0	66.2
9e	34.3	78.7	24.7	63.8
9f	33.4	80.1	24.4	63.7
9g	31.3	78.8	25.7	68.0
9h	31.5	82.4	24.1	64.8
9i	33.3	82.5	26.0	63.8

Table 4
The calculated molecular descriptors for the ligands, **9a-i**.

Ligand	MW	HB Donor	HB Acceptor	Log P	PSA	Rot.Bond
9a	509.7	2	4.5	7.4	74.6	10
9b	509.7	2	4.5	7.4	76.4	10
9c	509.7	2	4.5	7.4	75.8	10
9d	539.7	2	5.2	7.6	83.3	12
9e	523.7	2	4.5	7.7	74.0	10
9f	523.7	2	4.5	7.7	74.4	10
9g	523.7	2	4.5	7.8	74.5	10
9h	523.7	3	3.5	8.0	60.0	9
9i	523.7	2	4.5	7.6	75.6	10

of the enzyme by the Lineweaver–Burk plot of 1/V versus substrate para nitrophenyl phosphate disodium salt and urea 1/[S] in the presence of different inhibitor concentrations gave a series of straight lines as shown in Fig. 6A. The results of compounds **9h** showed that compounds intersected within the second quadrant. The analysis showed that V_{max} decreased to new increasing doses of inhibitors on the other hand K_m remains the same. This behavior indicates that compounds **9h** inhibit the alkaline phosphatase non-competitively to form enzyme inhibitor complex. Secondary plot of slope against the concentration of inhibitors showed enzyme-inhibitor dissociation constant (K_i) Fig. 6B. The kinetic results are presented in the Table 2.

3.5. Hemolytic activity

All the synthesized compounds, **9(a-i)**, were also subjected to hemolytic assay to find out their cytotoxicity profile. Results of percentage hemolysis are shown in Table 1. Our results showed that all compounds of this series have lower toxicity towards red blood cell membrane. Maximum membrane toxicity was shown by the compound **9i** (20.00 %) while minimum toxicity was recorded in **9h** (10.33 %). Precisely, a low toxicity was observed for molecule **9c** (12.40 %), **9a** (12.77 %), **9e** (13.77 %), **9d** (14.00 %), **9b** (15.40 %), **9f** (17.00 %) and **9g** (17.22 %) relative to Triton-X having % hemolysis of 45.32 %.

3.6. Molecular modeling of *9a-i* against alkaline phosphatase

The molecules were docked at the peripheral site of Placental alkaline phosphatase (PLAP) because the compounds undergo non-competitive inhibition. This peripheral site in PLAP is fully conserved in intestinal alkaline phosphatases (IAP) [50]. The molecules show plausible binding modes. Considering **9h**, the molecule occupies the binding site. The phenyl moiety on the triazole occupies a slightly hydrophobic loop whiles the amine portion of the molecule occupies a slightly hydrophilic cleft. The amide moiety of **9h** forms hydrogen bond with the side chain carbonyl oxygen of glutamic acid (Glu290). The phenyl group on the triazole moiety forms ##### stack with backbone carbonyl group of Leucine (Leu253). The molecule can also interact with methionine (Met254). The activity of these compounds is influence by steric factors. The amide portion of the active compounds fits into a slightly hydrophilic cleft whiles the inactive compounds pose on top of the cleft. These binding modes are shown in Figs. 7 and 8. The 2D graphical depiction of all the other docking complexes is mentioned in the supplementary file (Fig. S20–S27).

3.6.1. Chemical space

The calculated molecular descriptors molecular weight (MW), octanol/water partition coefficient (log *P*), hydrogen bond donor (HD), hydrogen bond acceptor (HA), polar surface area (PSA) and rotatable bonds (RB) are given in Table 3. The MW of the ligands is between 509.7 and 539.7g mol^{-1} and the log *P* values lie in the range of 7.4 and 8.3 whiles the PSA is between 59.9 and 83.3 Å [51,52]. These values demonstrate the compounds are in a favourable area of chemical space for further development (Table 4).

4. Conclusion

By using a convergent methodology, to synthesized the indole-triazole hybrids bearing *N*-substituted butanamides (**9a-i**) in excellent yields and their structure were confirmed by IR, ^{1}H NMR, ^{13}C NMR, EI-MS and CHN analysis data. These molecules exposed efficient potentials against alkaline phosphatase enzyme and depicted lower IC_{50} values relative to standard used potassium dihydrogen phosphate (KH_2PO_4). Thereinto, compound **9h** was found to be the most active compound ($IC_{50} = 0.062 \pm 0.017$ μM), and its inhibitory activity is about 10 times higher than potassium dihydrogen phosphate (KH_2PO_4) ($IC_{50} = 5.251 \pm 0.468$ μM). Moreover, all the compounds were attributed with mild hemolysis. Molecular modeling docked at the peripheral site of placental alkaline phosphatase (PLAP) was also used to assess the binding mode of the most potent inhibitors in the binding pocket of alkaline phsophatase. The kinetics mechanism was exposed by lineweaver-burk plots which revealed that, **9h**, inhibited alkaline phosphatase non-competitively by forming an enzyme inhibitor complex. The inhibition constants Ki calculated from Dixon plots for this compound was 0.045 μM. The computational ascription was also persuasive with the experimental results and these molecules disclosed good results of all scoring functions and interactions, which suggested a good binding to alkaline phosphatase. So, it was summated that these bi-heterocyclic butanamide derivatives might lead to further research gateways for drug designing and obtaining better and safe therapeutic agents for alkaline phosphatase-associated disorders, particularly, normal calcification of bones and teeth.

CRediT authorship contribution statement

Shakila: Writing – original draft. **Muhammad Athar Abbasi:** Validation. **Aziz-ur-Rehman:** Writing – review & editing. **Sabahat Zahra Siddiqui:** Conceptualization. **Majid Nazir:** Writing – review & editing. **Hussain Raza:** Formal analysis. **Syed Adnan Ali Shah:** Formal analysis. **Daniel Moscoh Ayine-Tora:** Formal analysis. **Muhammad Shahid:** Formal analysis. **Song Ja Kim:** Visualization.

Declaration of competing interest

The authors declare that they have no known competing financial interests or personal relationships that could have appeared to influence the work reported in this paper.

Data availability

Data will be made available on request.

Acknowledgement

The authors acknowledge the funding from the ORIC office of the Government College University Lahore vide Notification No. 21/ORIC/24 dated 04-01-2024.

Supplementary materials

Supplementary material associated with this article can be found, in the online version, at doi:10.1016/j.molstruc.2024.139649.

References

[1] P. Hardik, N. Darji, J. Pillai, B. Patel, Recent advances in the anticancer activity of indole derivatives, Int. J. Drug Res. Tech. 3 (2012) 225–230.
[2] M. Pinart, F. Kunath, V. Lieb, I. Tsaur, B. Wullich, S. Schmidt, German prostate cancer consortium (DPKK), Prognostic models for predicting overall survival in metastatic castration-resistant prostate cancer: a systematic review, World J. Urol. 38 (2020) 613–635.
[3] M.J. van der Doelen, P.N. Mehra, R. Hermsen, M.J.R. Janssen, W.R. Gerritsen, I. M. van Oor, Patient selection for radium-223 therapy in patients with bone metastatic castration-resistant prostate cancer: new recommendations and future perspectives, Clin. Genitourin. Cancer 17 (2019) 79–87.
[4] C. Laura, P. Cassanello, F. Muñiz, M.J. de Castro, M.L. Couce, Neonatal lethal hypophosphatasia: a case report and review of literature, Medicine (Baltimore) 48 (2018) e13269.
[5] C. Laura, A. Nardi, V. Ronca, P. Invernizzi, G. Mells, M. Carbone, Prognostic models in primary biliary cholangitis, J Autoimmun. 95 (2018) 171–178.
[6] A. Daniel, S. Gonzalo, R. Villa-Bellosta, Tissue non-specific alkaline phosphatase and Vascular Calcification: a potential therapeutic target, Curr. Cardiol. Rev. 15 (2019) 91–95.
[7] B. Allison L, C.M. Brown, Alkaline phosphatase: a potential biomarker for stroke and implications for treatment, Metab. Brain Dis. 34 (2019) 3–19.
[8] H. Daniel, Bruland, T.A. Guise, H. Suzuki, O. Sartor, Alkaline phosphatase in metastatic castration-resistant prostate cancer: reassessment of an older biomarker, Future Oncol. 24 (2018) 2543–2556.
[9] M. Makoto, S. Harajiri, S. Tabata, N. Yukimasa, Y. Muramoto, T. Komoda, Alkaline phosphataseactivity in blood group B or O secretors is fluctuated by the dinner intake of previous night, Rinsho. Byori. 4 (2013) 307–312.
[10] R.J. Masrour, S. Mahjoub, Quantification and comparison of bone-specific alkaline phosphatase with two methods in normal and paget's specimens, Caspian J. Intern. Med. 3 (2012) 478–483.
[11] M.A. emsp14D, J. emsp14E Moses, Click chemistry and medicinal chemistry; a case of cyclo-addiction, Chem. Med. Chem. 3 (2008) 715–723.
[12] H. Jingli, X. Liu, J. Shen, G. Zhao, P.G. Wang, The impact of click chemistry in medicinal chemistry, Expert Opin. Drug Discov. 7 (2012) 489–501.
[13] L. Roman, O. Vladzimirska, S. Holota, L. Zaprutko, A. Gzella, New 5-substituted thiazolo [3,2-b][1,2,4]triazol-6-ones: synthesis and anticancer evaluation, Eur. J. Med. Chem. 42 (2007) 641–648.
[14] T. Zitouni, Gülhan, Z.A. Kaplancikli, K. Erol, F.S. Kilic, Synthesis and analgesic activity of some triazoles and triazolothizdiazines, Farmaco 54 (1999) 218–223.

[15] T. Zitouni, Gülhan, Z.A. Kaplancikli, A. Özdemir, P. Chevallet, H.B. Kandilci, B. Gümüsel, Studies on 1,2,4-triazole derivatives as potential anti-inflammatory agents, Arch. Pharm. Chem. Life Sci. 340 (2007) 586–590.
[16] M. Mohammad, T. Akbarzadeh, V. Sheibani, M. Abbasi, L. Firoozpour, S. A. Tabatabai, A. Shafiee, A. Foroumadi, Synthesis of two novel 3-Amino-5-[4-chloro-2-phenoxyphenyl]-4*H*-1,2,4-triazoles with anticonvulsant activity, Iran. J. Pharm. Res. 9 (2010) 65–269.
[17] T. Christian W.C. Christensen, M. Meldal, Peptidotriazoles on solid phase: (1,2,3)-triazoles by regiospecific copper (I)-catalyzed 1,3-dipolar cycloadditions of terminal alkynes to azides, J. Org. Chem. 67 (2002) 3057–3064.
[18] R. Folkert, F. Zhou, M. Girardot, G. Kern, C.J. Eyermann, N.J. Hales, R.R. Ramsay, M.B. Gravestock, Identification of 4-substituted 1,2,3-triazoles as novel oxazolidinone antibacterial agents with reduced activity against monoamine oxidase A, J. Med. Chem. 48 (2005) 499–506.
[19] L. Wen-Tai, W.H. Wu, C.H. Tang, R. Tai, S.T. Chen, One-pot tandem copper-catalyzed library synthesis of 1-thiazolyl-1,2,3-triazoles as anticancer agents, ACS Comb. Sci. 13 (2010) 72–78.
[20] M. Sunny, S.I. Khan, D.S. Rawat, Synthesis of 4-aminoquinoline-1,2,3-triazole and 4-aminoquinoline-1,2,3-triazole-1,3,5-triazine hybrids as potential antimalarial agents, Chem. Biol. Drug Des. 78 (2011) 124–136.
[21] S. Deniz, A. Uzgoren-Baran, B.C. Tel, E.I. Somuncuoglu, I. Kazkayasi, K. Ozadali-Sari, O. Unsal-Tan, G. Okay, M. Ertan, B. Tozkoparan, Novel thiazolo (3,2-b)-1,2,4-triazoles derived fromnaproxen with analgesic/anti-inflammatory properties: synthesis, biological evaluation and molecular modeling studies, Bioorg. Med. Chem. 23 (2015) 2518–2528.
[22] N. Sirassu, N.S. Kumar, B.K. Swamy, N.V. Reddy, S.K. Althaf Hussain, M. Srinivasa Rao, Indole-2-carboxylic acid derived mono and bis 1,4-disubstituted 1,2,3-triazoles: synthesis, characterization and evaluation of anticancer, antibacterial, and DNA-cleavage activities, Bioorg. Med. Chem. Lett. 26 (2016) 1639–1644.
[23] M.B. Doğru, M.E. Mert, G. Kardaş, B. Yazıcı, Experimental and theoretical investigation of 3-amino-1,2,4-triazole-5-thiol as a corrosion inhibitor for carbon steel in HCl medium, Corros. Sci. 53 (2011) 4265–4272.
[24] A.R. Prasad, A.N. Rao, T. Ramalingan, P.B. Sattur, Synthesis and biological activity 4-amino-3-aryloxyalkyl-5-mercapto-1,2,4- triazoles, Ind. Drugs 25 (1998) 301–304.
[25] D.M. Zaher, M.I. El-Gamal, H.A. Omar, S.N. Aljareh, S.A. Al-Shamma, A.J. Ali, S. Zaib, J. Iqbal, Recent advances with alkaline phosphatase isoenzymes and their inhibitors, Arch. Pharm. 353 (2020) e2000011.
[26] F. Andrew, M.K. Jay, W.P.Z.Z. Zhang, J. Cohen, S. Lundeen, K. Rudnick, Y. Zhu, R. Winneker, Novel 5-Aryl-1,3-dihydro-indole-2-thiones: potent, orally active progesterone receptor agonists, Bioorg. Med. Chem. Lett. 13 (2003) 1317–1320.
[27] M.A. Abbasi, M. Nazir, Aziz ur-Rehman, S.Z. Siddiqui, M. Hassan, H. Raza, S.A. A. Shah, M. Shahid, S.Y. Seo, Bi-heterocyclic benzamides as alkaline phosphatase inhibitors: mechanistic comprehensions through kinetics and computational approaches, Arch. Pharm. Chem. Life Sci. (Archiv der Pharmazie) 352 (2019) 1800278.
[28] K. Imtiaz, M. Hanif, M.T. Hussain, A.A. Khan, M. Adil, S. Aslam, N.H. Rama, J. Iqbal, Synthesis, acetylcholinesterase and alkaline phosphatase inhibition of some new 1,2,4-triazole and 1,3,4-thiadiazole derivatives, Aus. J. Chem. 10 (2012) 1413–1419.
[29] I. Aliya, S. Zaib, F. Jabeen, J. Iqbal, A. Saeed, Unraveling the alkaline phosphatase inhibition, anticancer, and antileishmanial potential of coumarin–triazolothiadiazine hybrids: design, synthesis, and molecular docking analysis, Arch. Pharm. Chem. Life Sci. 349 (2016) 553–565.
[30] K.S. Munawar, S. Ali, M.N. Tahir, N. Khalid, Q. Abbas, I.Z. Qureshi, S. Shahzadi, Investigation of derivatized schiff base ligands of 1,2,4-triazole amine and their oxovanadium (IV) complexes: synthesis, structure, DNA binding, alkaline phosphatase inhibition, biological screening, and insulin mimetic properties, Russ. J. Gen. Chem. 9 (2015) 2183–2197.
[31] W. Khan, M.A. Abbasi, Aziz-ur Rehman, S.Z. Siddiqui, M. Nazir, S.A.A. Shah, H. Raza, M. Hassan, M. Shahid, S.Y. Seo, Convergent synthesis, free radical scavenging, Lineweaver-Burk plot exploration, hemolysis and *in silico* study of novel indole-phenyltriazole hybrid bearing acetamides as potent urease inhibitors, J. Heterocyclic Chem. 57 (2020) 2955–2968.
[32] M. Nazir, M.A. Abbasi, S.Z. Siddiqui, H. Raza, M. Hassan, S.A.A. Shah, M. Shahid, S.Y. Seo, Novel indole based hybrid oxadiazole scaffolds with *N*-(substituted phenyl)butanamides: synthesis, lineweaver–burk plot evaluation and binding analysis of potent urease inhibitors, RSC Adv. 8 (2018) 25920–25931.
[33] M. Nazir, M.A. Abbasi, S.Z. Siddiqui, K.M. Khan, Kanwal, U. Salar, M. Shahid, M. Ashraf, M.A. Lodhi, F.A. Khan, New indole-based hybrid oxadiazole scaffolds with *N*-substituted acetamides: as potent anti-diabetic agents, Bioorg. Chem. 81 (2018) 253–263.
[34] I. Zafar, Z. Ashraf, M. Hassan, Q. Abbas, E. Jabeen, Substituted phenyl [(5-benzyl-1,3,4-oxadiazol-2-yl)sulfanyl]acetates/acetamides as alkaline phosphatase inhibitors: synthesis, computational studies, enzyme inhibitory kinetics and DNA binding studies, Bioorg. Chem. 90 (2019) 103–108.
[35] S. Aamer, G. Saddique, P.A. Channar, F.A. Larik, Q. Abbas, M. Hassan, H. Raza, T. A. Fattah, S.Y. Seo, Synthesis of sulfadiazinyl acyl/aryl thiourea derivatives as calf intestinal alkaline phosphatase inhibitors, pharmacokinetic properties, lead optimization, Lineweaver-Burk plot evaluation and binding analysis, Bioorg. Med. Chem. 26 (2018) 3707–3715.
[36] A.R.S. Butt, M.A. Abbasi, Aziz-ur-Rehman, S.Z. Siddiqui, S. Muhammad, H. Raza, S. A.A. Shah, M. Shahid, A.G. Alsehemi, S.J. Kim, Convergent synthesis, kinetics insight, and allosteric computational ascriptions of thiazole-(5-aryl)oxadiazole hybrids embraced with propanamides as alkaline phosphatase inhibitors, RSC Adv. 13 (2023) 13798–13808.
[37] S. Poonam, J.D. Sharma, In vitro hemolysis of human erythrocytes by plant extracts with antiplasmodial activity, J. Ethnopharmacol. 74 (2001) 239–243.
[38] W.A. Powell, C.M. Catranis, C.A. Maynard, Design of self-processing antimicrobial peptide for plant protection, Lett. Appl. Microbiol. 31 (2000) 163–168.
[39] X.Z. Zhao, E. Kiselev, G.T. Lountos, W. Wang, J.E. Tropea, D. Needle, T.A. Hilimire, J.S. Schneekloth Jr, D.S. Waugh, Y. Pommier, T.R. Burke Jr, Small molecule microarray identifies inhibitors of tyrosyl-DNA phosphodiesterase 1 that simultaneously access the catalytic pocket and two substrate binding sites, Chem. Sci. 12 (2021) 3876–3884.
[40] B. Helen, M.J. Westbrook, Z. Feng, G. Gilliland, T.N. Bhat, H. Weissig, I. N. Shindyalov, P.E. Bourne, The protein data bank, Nucleic Acids Res. 28 (2000) 235–242.
[41] B. Helen, K. Henrick, H. Nakamura, Announcing the worldwide protein data bank, Nat. Struct. Mol. Biol. 10 (2003) 980.
[42] Scigress: Version FJ 2.6 (EU 3.1.7) Fijitsu Limited, 2008–2016.
[43] G. Jones, P. Willett, R.C. Glen, A.R. Leach, R. Taylor, Development and validation of a genetic algorithm for flexible docking, J. Mol. Biol. 267 (1997) 727–748.
[44] E. Matthew, D.C.W. Murray, T.R. Auton, G.V. Paolini, R.P. Mee, Empirical scoring functions: I. The development of a fast empirical scoring function to estimate the binding affinity of ligands in receptor complexes, J. Comput. Aided Mol. Des. 11 (1997) 425–445.
[45] L.V. Marcel, J.C. Cole, M.J. Hartshorn, C.W. Murray, R.D. Taylor, Improved protein–ligand docking using GOLD, Proteins 52 (2003) 609–623.
[46] K. Oliver, T. Stutzle, T.E. Exner, Empirical scoring functions for advanced protein−ligand docking with PLANTS, J. Chem. Inf. Model. 49 (2009) 84–96.
[47] T.M. Wijnand, M.L. Verdonk, General and targeted statistical potentials for protein–ligand interactions, Proteins 61 (2005) 272–287.
[48] QikProp Version 3.2, Schrodinger, New York, 2009.
[49] Leukothea, L. Thoukydidis, A. Mirza, S. Naeem, J. Reynisson, Benchmarking the reliability of QikProp. Correlation between experimental and predicted values, J. QSAR Comb. Sci. 27 (2008) 445–456.
[50] L. Paola, E.A. Stura, A. Ménez, Z. Kiss, T. Stigbrand, J.L. Millán, M. Hélène Le Du, Structural studies of human placental alkaline phosphatase in complex with functional ligands, J. Mol. Bio. 350 (2005) 441–451.
[51] F. Zhu, G. Logan, Reynisson, J. Mol. Inf. 31 (2012) 847–855.
[52] H. Aslan, F. Yetişsin, A. Korkmaz, E. Bursal, Design, synthesis, characterization, enzyme inhibition, molecular docking, and pharmacological evaluation of new chalcone-sulfonate derivatives bearing thiophene, ChemistrySelect 9 (2024) e202400053, https://doi.org/10.1002/slct.202400053.